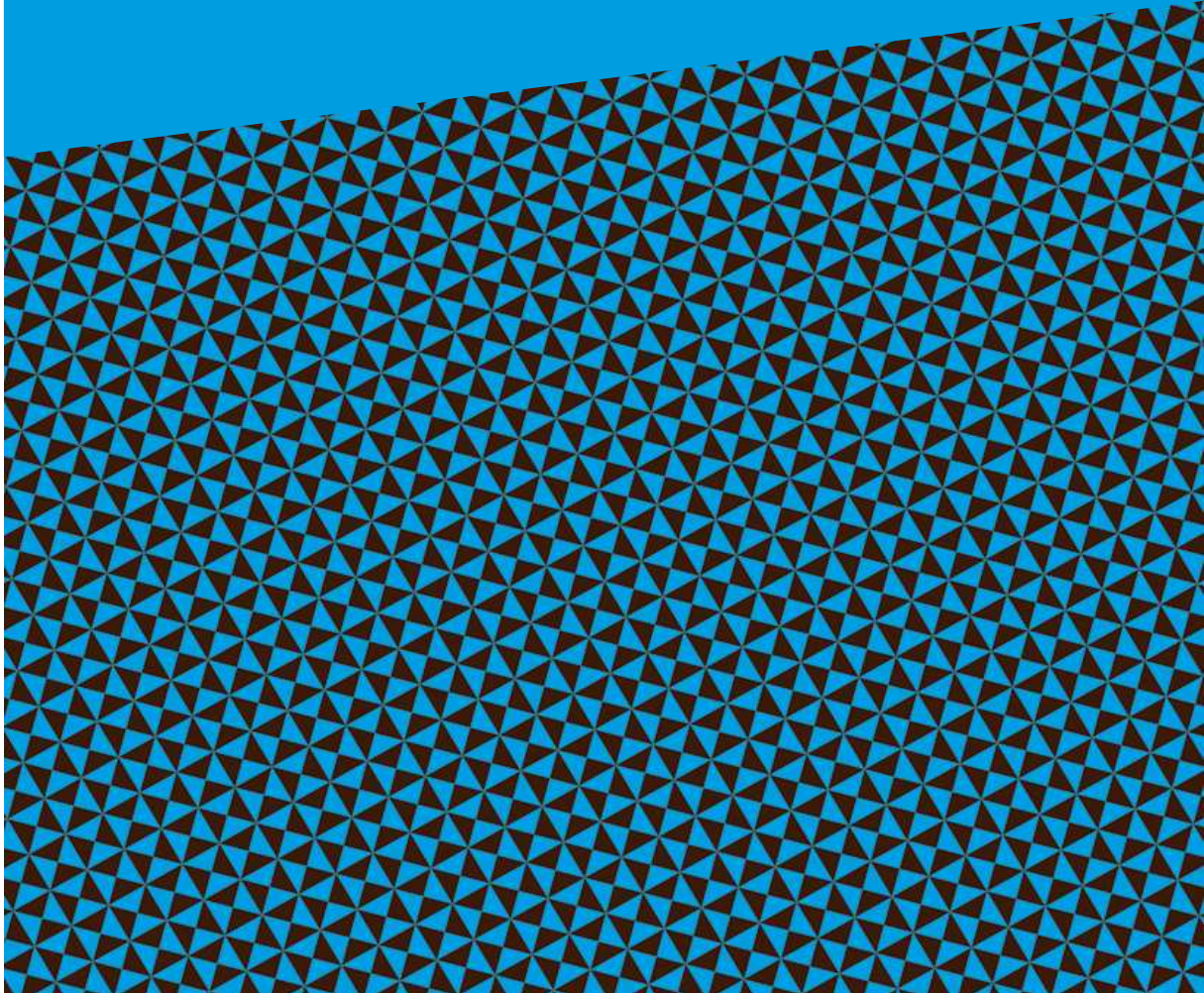


# **Book of Abstracts of the Workshop**

**Hydrodynamics at small scales: from soft  
matter to bioengineering**

**June 14-16, 2023  
University of Bordeaux, building B6  
Talence (FRANCE)**



---

# Lift at low Reynolds number

Thomas Salez\*<sup>1</sup>

<sup>1</sup>Laboratoire Ondes et Matière d'Aquitaine – Centre National de la Recherche Scientifique : UMR5798,  
Université de Bordeaux : UMR5798, Université de Bordeaux, Centre National de la Recherche  
Scientifique – France

## Abstract

Soft and wet contact arises in a range of phenomena that spans many length and time scales, and includes: landslides, aquaplaning of tires, wear of industrial bearings, ageing of synovial and cartilaginous joints, cell motion in blood vessels or microfluidic devices, and atomic-force or surface-force rheology. Therein, the coupling between boundary elasticity and confined viscous flow leads to a striking zoology of counterintuitive emergent effects. From the canonical situation of a free particle that can simultaneously sediment, slide, and roll in a viscous fluid, and near a soft wall, we study a range of novel inertial-like (despite the low-Reynolds-number flow) features, such as: enhanced sedimentation, elastohydrodynamic bouncing, roll reversal, emergent lift and torque, dynamical adhesive-like forces...

---

\*Speaker

# Dynamics of Collision of Two Arbitrarily Placed Evaporating Drops

Ashwani Kumar Pal<sup>1</sup> and Gautam Biswas<sup>2</sup>

<sup>1</sup> Department of Mechanical Engineering, IIT Kanpur, 208016, Kanpur, India, pashwani@iitk.ac.in

<sup>2</sup> Department of Mechanical Engineering, IIT Kanpur, 208016, Kanpur, India, gtm@iitk.ac.in

The collision of two or more drops is a very interesting area of study because it is commonly encountered in many industrial processes, such as the combustion and spray drying. Collision of drops is also encountered in many environmental situations including the rainfall. The outcome of the binary collision of the drops may be different depending on the effects of relevant physical parameters, such as the Weber number ( $We = 2\rho_l U^2 R / \sigma$ ) and Ohnesorge number ( $Oh = \mu_l / \sqrt{\rho_l R \sigma}$ ). Where,  $\rho_l$  is the density of drop fluid,  $\sigma$  is the coefficient of surface tension,  $R$  is the radii of the drops and  $U$  is the relative velocity between the drops. There are five known possible outcomes of the drop collision in the case of identical viscosities of the drop-liquids [1]. These are (a) slow coalescence, (b) bouncing, (c) fast coalescence, (d) reflexive separation, and (e) stretching separation. The reflexive separation takes place in the case of a head on collision of the drops where the fluid motion stretches the liquid volume into two parts forming a ligament in between. This ligament stretches out and breaks due to outward moment of the liquid packets giving rise to two drops and one relatively smaller sized drop called the satellite drop. The formation of a satellite drop is affected as we move away from the symmetrical binary collision [2]. Contrary to reflexive separation, the stretching separation takes place in the case of an oblique collision of the drops where a relatively smaller regions of the drops interact with each other [3]. The process of interaction between the drops is affected by the evaporation in the presence of warm ambience and vice versa.

The analyses of different outcomes of binary collision of the drops during bouncing, reflexive, and stretching separation regimes are performed using detailed numerical simulations. A finite difference-based solution procedure which incorporates a coupled level-set and volume-of-fluid (CLSVOF) method-based interface capturing technique [4] is deployed to simulate the processes. A concentration gradient driven mass transfer model [4] is coupled with the flow solver to capture the evaporation of the drops in the hot gas. Additionally, a vapor diffusion equation is solved to track the concentration of the vapor in the drop ambience. The solver has been tested by considering different benchmark problems to verify the mass transfer from the evaporating drops.

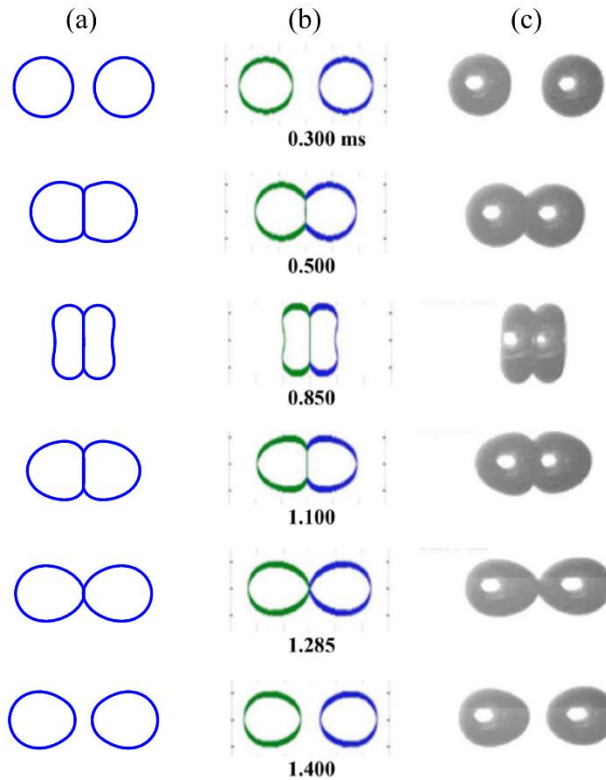


FIG 1. Comparison of the results obtained for droplet bouncing. (a) Present simulations, (b) simulation results of Pan et al. [5], and (c) experimental results of Pan et al [5].

The collision dynamics of two tetradecane drops in air in the bouncing regime is simulated and the results obtained through our simulation are compared with the numerical and experimental results of Pan et al [5]

(Figure 1). The simulations are performed in an axisymmetric domain with two identical drops with radius  $167.6 \mu\text{m}$  and relative velocity of  $U = 0.992 \text{ m/s}$ . The corresponding Weber number and Ohnesorge number are  $9.629$  and  $0.0356$ . It can be observed from Figure 1 that the drops bounce back since they do not have large inertia to overcome the capillary force. The droplets undergo significant deformation before bouncing, and this process is term as the hard collision.

We consider another case of binary collision of two identical drops to show the reflexive separation with formation of one satellite drop. Collision of two tetradecane drops of radii  $150 \mu\text{m}$  and the relative velocity  $2.29 \text{ m/s}$  is simulated for this purpose. The pertinent governing parameters for this case are  $We = 45.92$  and  $Oh = 0.0376$ . In this case, the drops separate out after collision since they have high inertia to overcome the capillary forces. The Weber number is higher than the earlier case of bouncing. Figure 2 reveals that a thin ligament is formed in between the two stretched out liquid masses. As a consequence, the ligament, connecting these masses, is pulled away. The pinch off takes place at two ends of the ligament giving rise to the satellite drop as observed by Huang et al [2].

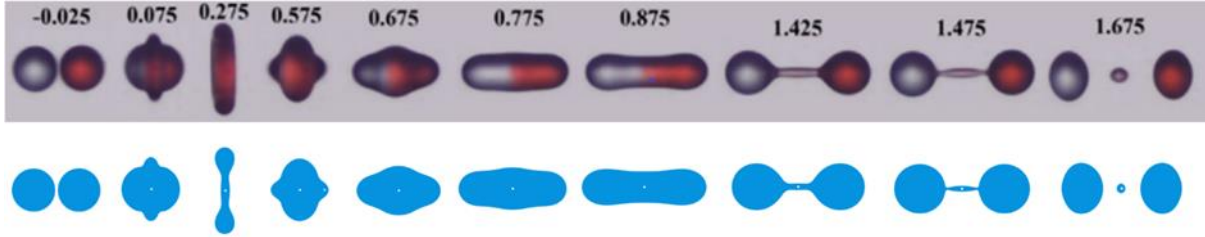


FIG 2. Comparison of reflexive separation of two tetradecane drops. Top panel shows numerical results of Huang et al. [2] while the bottom panel shows results due to present simulation.

It is further observed that as the collision process moves away from symmetric collision, the formation of the satellite drop does not happen anymore. The outcomes of the collision process of two tetradecane drop having a radius ratio of  $1.28$  are shown in Figure 3. All other physical parameters used for the simulation are same as those used for Figure 2. It is evident that the formation of satellite drop does not take place due to asymmetry in the sizes of the drops [2].

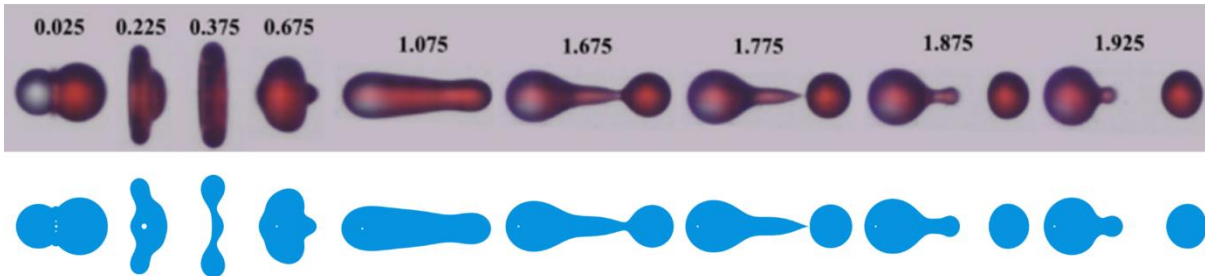


FIG 3. Comparison of reflexive separation of two tetradecane drops having a radius ratio of  $1.28$ . Top panel shows numerical results of Huang et al. [2] while the bottom panel shows results due to present simulation.

- 
- [1] K. H. Al-Diwari and A. E. Bayly, A new model for the bouncing regime boundary in binary droplet collisions, *Phys. Fluids* **31**, 027105 (2019).
  - [2] K. L. Huang, K. L. Pan, and C. Josserand, Pinching dynamics and satellite droplet formation in symmetrical droplet collisions, *Phys. Rev. Lett.* **123**, 234502 (2019).
  - [3] G. S. Chaitanya, K. C. Sahu, and G. Biswas, A study of two unequal-sized droplets undergoing oblique collision, *Phys. Fluids* **33**, 022110 (2021).
  - [4] A. K. Pal and G. Biswas, Accurate prediction of transport coefficient of an evaporating liquid drop, *J. Heat and Mass Transfer* **145**, 041602-1 (2023).
  - [5] K. L. Pan, C. K. Law, and B. Zhou, Experimental and mechanistic description of merging and bouncing in head-on binary droplet collision, *J. Appl. Phys.* **103**(6), 064901(2018).

# Abstract: Indo French Workshop, Univ. Bordeaux

Uddipta Ghosh

Mechanical Engineering, IIT Gandhinagar

**Title of the presentation:** Electrophoresis in complex fluids: applications to separation processes.

It is well known that a number of biological and polymeric liquids exhibit non-Newtonian rheological characteristics and their rheologies are best described by viscoelastic constitutive models, that account for properties such as shear-thinning, non-zero normal stress coefficients, relaxation time scales, to underline a few. Flow of such complex fluids in narrow fluidic pathways, especially with the aid of externally imposed electric field are becoming increasingly prominent for their multifold applications in emerging fields such as sample detection and separation processes, genome sequencing etc. For instance, state-of-the art Polymerase chain reaction tests regularly use gel-electrophoresis to transport and visualize DNA fragments, where polymer gels are often deployed as the suspending medium. Yet, a comprehensive and first principle based description of electrically driven flows in complex fluidic media remains an important open question, that our work over the past several years has attempted to address.

We first develop a systematic analytical framework to investigate the flow patterns of a viscoelastic fluid near a charged surface, actuated by an externally imposed electric field. We confine our attention to the thin Electrical Double Layer limit and establish that the “Smoluchowski Slip velocity”, which the bulk electro-neutral fluid experiences as an effective slip at the solid boundary, gets fundamentally modified in a viscoelastic medium as it becomes a “non-local” phenomena - i.e., it depends on the derivative of the surface potential. When this same principle is applied to flows over curved and arbitrarily charged surfaces, it is noted that the resulting slip velocity depends on the curvature, the derivatives of the surface charge w.r.t to the surface coordinates as well as the motion of the surface itself - all of these are in stark contrast to the well-established Newtonian theory.

We subsequently apply this effective velocity boundary condition to compute the electrophoretic mobility of non-uniformly charged spherical particles in viscoelastic fluids and demonstrate that the particles’ angular and translational velocities strongly depend on their sizes, even when they carry weak surface charge. Such a physical paradigm, which leads to a breaking of foreaft symmetry, is unique to complex fluids despite operating in the regime of creeping flows.

We have further expanded upon the above results to envisage a semi-analytical generic framework for tracing the trajectories of particles suspended in viscoelastic media and carrying arbitrary non-uniform charge densities, using their instantaneous translational velocity and accounting for the temporal evolution of their surface charge driven by rotation. The framework also takes into account the possible presence of externally imposed flows.

We illustrate that in a quiescent complex fluidic media, non-uniformly charged particles may generally follow distinct trajectories depending on their sizes, thus signaling a significant shift from the classical Newtonian paradigm. We demonstrate that the final steady state trajectory of the particle and its possible migration away from the direction of the electric field is largely governed by its size, the multipole moments of its surface charge, their mutual interactions and especially the presence of non-zero quadrupole moments. We envision that this size dependent electrophoretic migration can become an effective tool for separating and sorting charged entities in small scale devices using complex fluids as the suspending medium.

On the other hand, the presence of an externally imposed steady shear flow may drastically alter the electrophoretic trajectory of the particle. First, it is established that depending on the strength of the shear flow, the particle may either end up with a steady orientation or, may oscillate around a non-linear center in the phase space. While in Newtonian fluids, non-zero quadrupole

moment is still required to cause cross-stream migration, the sustained rotation caused by the external flow in a viscoelastic media may actually cause intriguing migration patterns, even for particles only carrying axisymmetric surface charge. When the surface charge has a non-zero quadrupole moment, the nature of the trajectory may strongly depend on the relative strength of the imposed flow and the electrophoretic mobility.

# Droplet size distribution using in-line holography and machine learning

Someshwar Sanjay Ade<sup>1</sup>, Pavan Kumar Kirar<sup>2</sup>, Lakshmana Dora Chandrala<sup>3</sup> and Kirti Chandra Sahu<sup>2</sup>

<sup>1</sup>Center for Interdisciplinary Program, Indian Institute of Technology Hyderabad, 502 284, Telangana, India

<sup>2</sup>Department of Chemical Engineering, Indian Institute of Technology Hyderabad, 502 284, Telangana, India

<sup>3</sup>Department of Mechanical & Aerospace Engineering, Indian Institute of Technology Hyderabad, 502 284, Telangana, India

Email: [ksahu@che.iith.ac.in](mailto:ksahu@che.iith.ac.in)

Fragmentation of droplets and resulting size distribution of child droplets have a significant impact on various industrial applications like combustion, surface coating, pharmaceutical production, disease transmission modeling, and artificial rain technology. They also play a crucial role in understanding natural phenomena such as clouds and rainfall. Different modes of breakup, including vibrational, bag, bag-stamen, multi-bag, shear, and catastrophic modes, occur when a droplet is exposed to an airstream, leading to the competition between surface tension and aerodynamic forces. In this study, we use shadowgraphy and deep-learning-based digital in-line holography techniques (figure 1) to experimentally investigate the morphology and size distribution of satellite droplets resulting from the interaction of a freely falling water droplet with an airstream of different strengths. Our analysis reveals that in dual-bag fragmentation, the parent drop fragmentation contributes to the atomization of tiny child droplets, while core drop disintegration predominantly results in larger fragments (figure 2). Despite the complexity associated with dual-bag fragmentation, we demonstrate that it exhibits a bi-modal size distribution, whereas single-bag breakup undergoes a tri-modal size distribution. We also employ an analytical model developed by Jackiw and Ashgriz<sup>1,2</sup>, which convincingly predicts the experimentally observed droplet volume probability density. Our study further estimates the temporal evolution of child droplet production and confirms that the analytical model adequately predicts the droplet size distribution for a range of Weber numbers<sup>3,4</sup>.

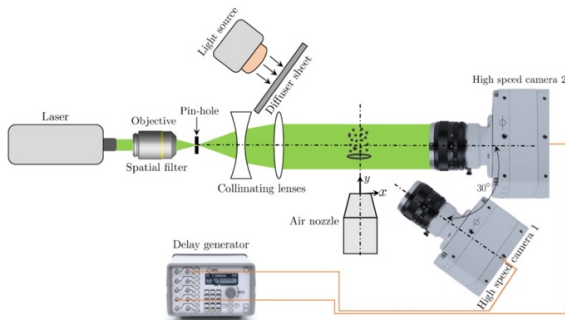


Figure 1: Schematic diagram of the experimental set-up (top view) involving shadowgraphy and deep-learning-based digital in-line holography techniques.

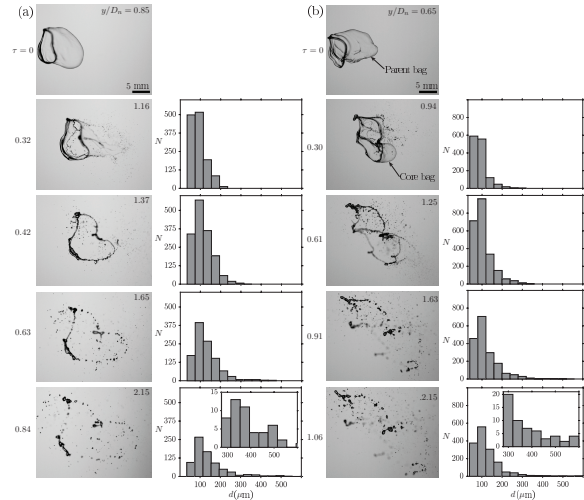


Figure 2: Temporal evolution of the fragmentation process (from shadowgraphy) and droplet size distribution (the droplet counts,  $N$  versus the droplet diameter,  $d$ ) for (a)  $We = 12.6$  and (b)  $We = 34.8$ .

- 1) Jackiw, I. M. & Ashgriz, N. 2021 On aerodynamic droplet breakup. *J. Fluid Mech.* 913, A33.
- 2) Jackiw, I. M. & Ashgriz, N. 2022 Prediction of the droplet size distribution in aerodynamic droplet breakup. *J. Fluid Mech.* 940, A17.
- 3) Ade, S. S., Kirar, P. K., Chandrala, L. D. & Sahu, K. C. 2023 Droplet size distribution in a swirl airstream using in-line holography technique. *J. Fluid Mech.* 954, A39.
- 4) Ade, S. S., Chandrala, L. D. & Sahu, K. C. 2023 Size distribution of a drop undergoing breakup at moderate Weber numbers. *J. Fluid Mech.* 959, A38.

# Understanding the Impact Dynamics of Emulsions and Air-in-Liquid Compound Droplets

Deekshith Naidu P<sup>1</sup>, Srijan Kumar<sup>2</sup>, and Susmita Dash<sup>3</sup>

<sup>1</sup> *Department of Mechanical Engineering, Indian Institute of Science, Bangalore, India, 560012*  
*deekshithpn@iisc.ac.in*

<sup>2</sup> *Department of Mechanical Engineering, Indian Institute of Science, Bangalore, India, 560012*  
*srijank@iisc.ac.in*

<sup>3</sup> *Department of Mechanical Engineering, Indian Institute of Science, Bangalore, India, 560012*  
*susmitadash@iisc.ac.in*

The impact of droplets on substrates are relevant in applications ranging from spray cooling, biological cell printing, additive manufacturing to agricultural sprays. The impact of droplets on rigid substrates is accompanied by the outward spreading of the liquid on the substrate forming a lamella. Here, we report on the impact dynamics of an air-in-liquid hollow droplet on a rigid substrate. We show that during impact of a hollow droplet (HD), formation of the lamella is accompanied by the formation of a central jet of liquid (counterjet) moving upward against the direction of gravity. We experimentally investigate the influence of the size of the air bubble, liquid viscosity, and height of impact on the evolution of counterjet (CJ) and the spreading characteristics of the lamella. The volume of the CJ formed during the impact of a HD with a given liquid volume is observed to be independent of the height of impact and increases with the volume of air encapsulated in the HD. Interestingly, even though almost half of the liquid in the droplet goes into forming the counterjet, the maximum spread of a HD is almost similar to that of a simple droplet with liquid volume and height of impact same as that of the HD. We establish that the viscous losses during impact of a HD during the spreading phase are relatively less compared to a simple droplet. We propose a model to predict the maximum spread during the impact of a hollow droplet based on the energy interaction between the spreading liquid and the liquid in the counterjet during the impact process.

In applications such as spraying of pesticides, the retention of the droplets on the leaves is crucial. Here, we discuss the role of oil and added polymers in water on the impact dynamics on hydrophobic substrates. We also present a timescale analysis to describe the retardation in the rate of retraction during impact of droplets comprising water-oil-polymer emulsions on different substrates.

# On the jetting direction during the collapse of a bubble in contact with a wall

Daniel Fuster<sup>1</sup>, Mandeep Saini<sup>1</sup>, Erwan Tanne<sup>2</sup>, Stephane Zaleski<sup>1</sup> and Michel Arrigoni<sup>2</sup>

<sup>1</sup>Institut Jean Le Rond D'Alembert, CNRS/Sorbonne Université, Paris, France [fuster@dalembert.upmc.fr](mailto:fuster@dalembert.upmc.fr)

<sup>2</sup>ENSTA Bretagne UMR 6027 - IRDL F-29806, Brest, France, [Michel.Arrigoni@ensta-bretagne.fr](mailto:Michel.Arrigoni@ensta-bretagne.fr)

## I. INTRODUCTION

The dynamics of collapsing bubbles have been mainly investigated assuming spherical symmetry [1] however, in the presence of a nearby wall, the bubble response is no longer spherical and three dimensional effects must be taken into account [2, 3]. Most of theoretical and numerical studies in this later case focus on the dynamics of bubbles which are not in contact with the wall. In reality, it is well known that bubbles typically appear from defects present in a solid wall and bubbles are indeed in contact with the wall when they collapse. In this work we show that the bubble shape at the instant of maximum radius is a critical parameter determining the mechanical effects induced by the collapse of a bubble along the wall.

## II. NUMERICAL RESULTS

We present first some numerical results using the compressible solver available in Basilisk [1]. These results reveal the existence of different regimes of interaction between a non-spherical collapsing bubble and a wall [2]. We show how the effective contact angle at the instant of maximum expansion determines the mechanisms of interaction between the bubble and the wall. Using the results from the impulse theory, we show that for sufficiently flat bubbles the solution of the Euler equations is singular at the contact line. The existence of this singularity is shown to be responsible of high velocity jets parallel to the wall that eventually lead to the emission of vortices in direction opposite to the wall. The Direct Numerical Simulation of the Rayleigh collapse problem of spherical cap bubbles attached to a wall will be used to validate theoretical predictions and analyze the fully non-linear evolution of the bubble.

## III. EXPERIMENTAL RESULTS

Figure 1 shows the consequences of the collapse of a bubble in contact with a wall. By adding a small amount of ink at the bottom of the tank, we can visualize the formation of the vortex ring that forms after the collapse of a bubble generated by a laser pulse (see ref. [2] for details). As numerically predicted, the vortex propagates upwards and, when it reaches the free surface, generates a jet indirectly validating the results found numerically.

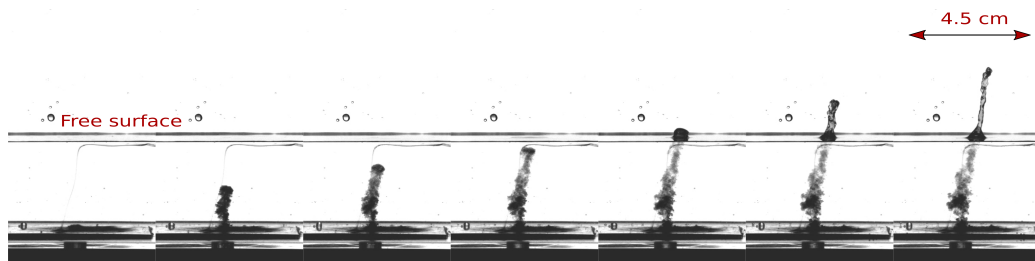


Figure 1: Formation of a vortex dipole from the collapse of a bubble at the bottom of a water filled tank

[1] D. Fuster and S. Popinet, An all-Mach method for the simulation of bubble dynamics problems in the presence of surface tension, *J. Comp. Phys.* **374**, 752 – 768 (2018).

[2] M. Saini, E. Tanne, M. Arrigoni, S. Zaleski and D. Fuster, On the dynamics of a collapsing bubble in contact with a rigid wall, *J. Fluid Mech.* **948**, 1 – 19 (2022).

# Self-organization and rheology of phoretic suspensions in shear flows

Prathmesh Vinze and Sebastien Michelin

*Laboratoire d'hydrodynamique, Ecole Polytechnique, Centre National de la Recherche Scientifique, Centre National de la Recherche Scientifique : UMR7646*

## Abstract

A Janus phoretic particle converts the chemical energy present in its environment to mechanical energy to self-propel. These active particles modify and respond to their hydrodynamic and chemical environment, thus allowing them to respond to an external flow and interact hydro-dynamically and chemically with other particles. These interactions are known to lead to non-trivial collective behavior within such biological or synthetic active suspensions (e.g., cluster formation of phoretic particles or bacterial swarming). Recent experiments and analysis have demonstrated that the response of active suspensions to shear flow is non-trivial and can, in fact, lead to a significant reduction in viscosity due to the injection of energy at the microscopic scale.

In this work, we numerically analyze the response to shear of a dilute and confined suspension of chemotactic phoretic particles using a continuum model of a dilute phoretic suspension (Fig.1). We show that a 1D transient steady distribution driven by the effect of confinement is a common feature for the confinement and shear rate intensities considered. This 1D state is stable for strong confinement and thus observed in the long-term dynamics for small channel widths. For wider channels, the transient state is unstable to streamwise perturbations due to the chemotactic instability, leading to particles' aggregates forming along the channel's walls. The relative arrangements of the aggregates on the two opposite walls are determined by the relative influence of shear intensity and chemotaxis and critically condition the suspension's

dynamics and particle-induced flow.

In a second step, we investigate the feedback effect on the flow of the self-organized suspension and, more specifically, on the effective viscosity of the suspension. We show that the induced flow and, consequently, its rheological behavior strongly depend on the self-organization regime. The most substantial reduction in viscosity is achieved for a weak shear case with the induced flow shown in Fig 2. The clockwise rotating vortices entrain the plate, thus reducing the required force at the plates to maintain a constant velocity.

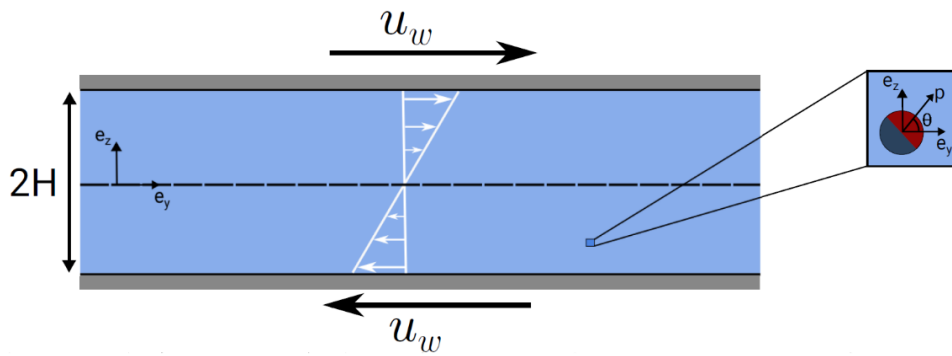


Figure 1

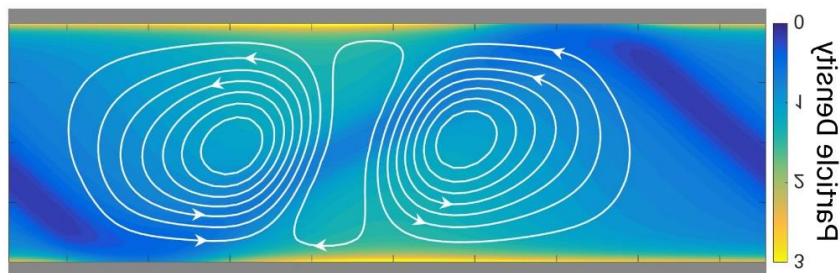


Figure 2

# Thin fluid film over a spherical surface: Contact line driven fingering instability

Ananthan Mohan and Gaurav Tomar\*

*Department of Mechanical Engineering, Indian Institute of Science, Bangalore*

E-mail: gtom@iisc.ac.in

## Abstract

Thin fluid films are extensively studied due to its ubiquitous nature in many industrial applications. While thin fluid film flows over flat surfaces are well studied and understood little work has been done in understanding film flows over curved surfaces. In this work we explore flow of a completely wetting Newtonian fluid over a spherical surface, with particular focus on contact line instabilities at the fluid front. Understanding contact line driven instability in this configuration has inherent difficulties due to the presence of curvature and divergent nature of the flow imposed by the geometry. In this study we derive a generalized<sup>1</sup> thin film equation based on long wave approximation for a fluid film on a spherical surface and using numerical simulations<sup>2</sup> we provide some basic insights into the flow dynamics. We observe that unlike thin film flow over flat surfaces the contact line driven instability is engendered multiple times as the flow progresses.

From the general thin film formulation using the metric coefficients for spherical surface, we have the thin fluid film equation on a spherical surface as,

$$\frac{\partial \bar{h}}{\partial t} + \frac{1}{3\mu \sin \vartheta} \frac{1}{R} \frac{\partial}{\partial \vartheta} \left( \sin \vartheta \bar{h}^3 \frac{\sigma \partial \bar{\kappa}}{R \partial \vartheta} + \rho g \sin \vartheta - \frac{\rho g \cos \vartheta}{R} \frac{\partial \bar{h}}{\partial \vartheta} \right) + \frac{1}{R} \frac{\partial}{\partial \varphi} \left( \bar{h}^3 \frac{1}{\sin \vartheta} \frac{1}{R} \frac{\partial \bar{\kappa}}{\partial \varphi} - \frac{\rho g \cos \vartheta}{R} \frac{\partial \bar{h}}{\partial \varphi} \right) = 0 \quad (1)$$

where

$$\bar{\kappa} = \frac{2\bar{h}}{R^2} + \frac{1}{\sin \vartheta} \frac{1}{R} \frac{\partial}{\partial \vartheta} \left( \frac{\sin \vartheta}{R} \frac{\partial \bar{h}}{\partial \vartheta} \right) + \frac{1}{R} \frac{\partial}{\partial \varphi} \left( \frac{1}{\sin \vartheta} \frac{1}{R} \frac{\partial \bar{h}}{\partial \varphi} \right) \quad (2)$$

Here  $\vartheta$  and  $\varphi$  represent the polar and azimuthal angles and  $R$  is the radius of the sphere. Here  $\bar{\kappa}$  represents the curvature of the fluid film and  $h$  is the height of the film. Dynamic viscosity of the fluid is  $\mu$  and surface tension constant is  $\sigma$  and density is given by  $\rho$ .

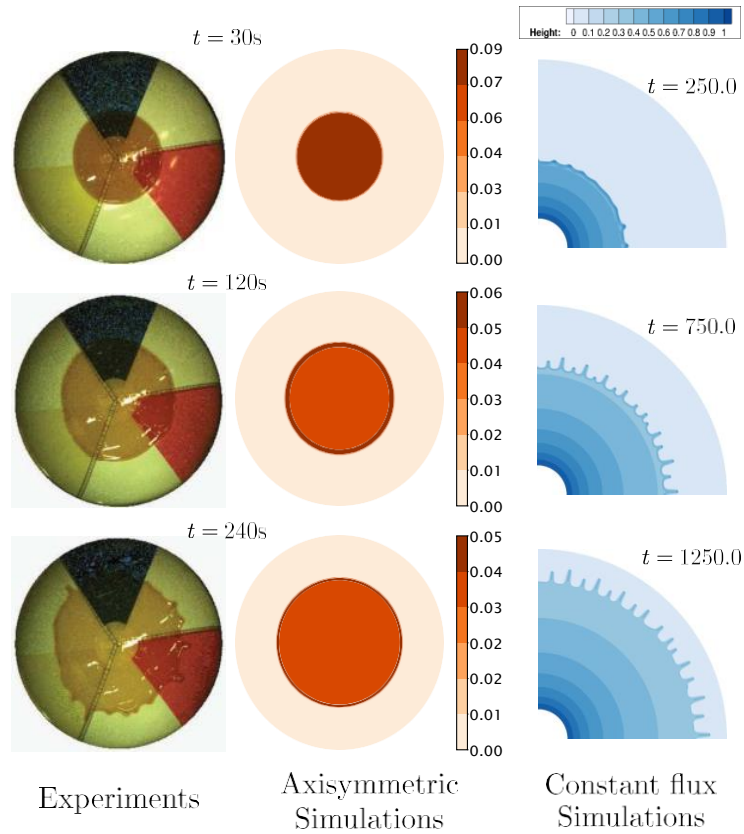


Figure 1: Numerical simulation of a thin fluid film over a spherical surface.

Assuming the initial spreading of the fluid is axisymmetric we can reduce the governing

equation as a function of time and polar angle. Assuming symmetric boundary conditions on top of the sphere and a precursor film ( $b \ll h$ ) as a boundary condition, we have used successive finite difference approximation to convert the governing partial differential equation to a set of ordinary differential equations which we solve using a fifth order accurate Backward Differentiation formulae-based solver.<sup>2</sup> These simulations match well with the experiments<sup>3</sup> as seen from figure 1.

In order to capture the fingering instability, we simulate the thin fluid film flow over a sphere where we maintain a constant height of the film with constant flow rate on top of the sphere and the initial front of the film is subjected to very small random perturbation. Figure 1 shows the numerical simulation of golden syrup of initial height  $0.034\text{cm}$  flowing over a sphere of radius,  $R = 24\text{cm}$ , with surface tension  $\sigma = 78\text{mN/m}$  and kinematic viscosity,  $\nu = 4.5 \times 10^2 \text{cm}^2/\text{s}$ . We use initial film height ( $h_0$ ) to non-dimensionalise the fluid film height, the spatial dimensions are non-dimensionalised using  $x_c = \left(\frac{\sigma h_0}{\rho g}\right)^{\frac{1}{3}}$ , and we use  $T = \frac{3\nu x_c}{gh_0^2}$  to non-dimensionalise the time. Unlike in the case of fluid film flow over a flat surface, due to the presence of varying components of gravity as flow progresses as well as divergent flow effects imposed by the geometry we observe contact line driven fingering instability multiple times as the flow progresses.

## References

- (1) Myers, T. G.; Charpin, J. P.; Chapman, S. J. The flow and solidification of a thin fluid film on an arbitrary three-dimensional surface. *Physics of Fluids* **2002**, *14*, 2788–2803.
- (2) Cohen, S. D.; Hindmarsh, A. C.; Dubois, P. F. CVODE, a stiff/nonstiff ODE solver in C. *Computers in physics* **1996**, *10*, 138–143.
- (3) Takagi, D.; Huppert, H. E. Flow and instability of thin films on a cylinder and sphere. *Journal of Fluid Mechanics* **2010**, *647*, 221–238.

# Acoustical tweezers: a new tool to probe soft and biological matter

Diego Baresch<sup>1</sup>

<sup>1</sup> Physical Acoustics Department, Institut de Mécanique et d'Ingénierie (I2M), Université de Bordeaux, France

The controlled manipulation of matter using the radiation pressure of light is well established as a powerful tool in the physical and biological sciences: “optical tweezers” use a single laser beam to trap and manipulate individual particles with precisely controlled forces. The piconewton force range and nanometer spatial resolution make optical tweezers ideally suited to probe biomolecular interactions, colloidal systems, organelles, and even living cells. Despite the wide applicability of optical tweezers in biological and soft matter physics, the challenge remains on probing bulk soft materials such as cell colonies or biological tissue, which require much larger stresses to be significantly deformed.

Using the radiation pressure of sound, rather than light, we have recently developed single-beam acoustical tweezers, which can trap elastic particles as large as 400 microns with forces up to the micronewton range, reducing the beam intensity by 5 orders of magnitude compared to their optical counterpart. The main characteristics of this technique open prospects to investigate mechanisms where large deformations and stresses are required, involving turbid or opaque-to-light media or requiring the gentle manipulation of fragile objects. We will present the basic physical mechanisms underpinning acoustical tweezers and their recent application to manipulate individual microbubbles involved in various biomedical applications of ultrasound.

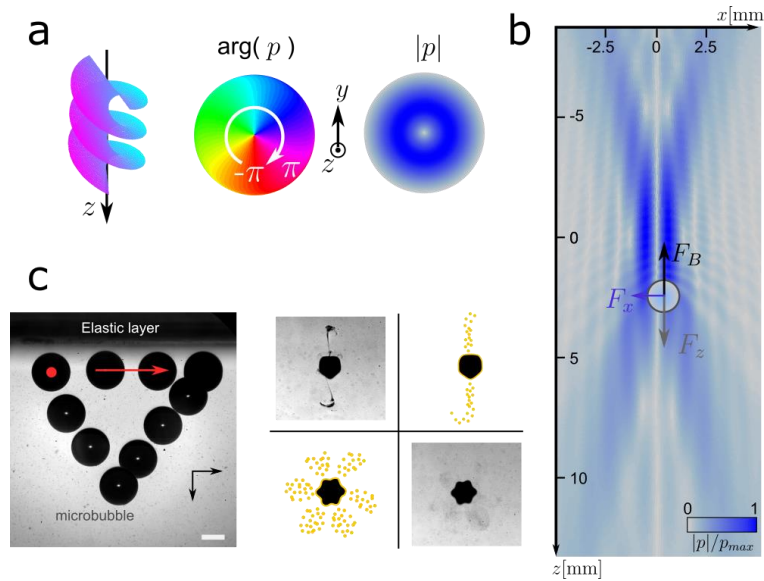


FIG. 1. Acoustical tweezers for microbubble manipulation. a) Helicoidal structure of the incident trapping beam (from left to right: wavefront, phase and magnitude). b) Numerical simulation of acoustic radiation forces acting on a microbubble interacting with the trapping beam. c) Photograph of the contactless microbubble manipulation with acoustical tweezers.

# Hydrodynamics of microlayer formation

Mandeep Saini<sup>1</sup>, Xiangbin Chen<sup>1</sup>, Stephane Zaleski<sup>1,2</sup> and Daniel Fuster<sup>1</sup>

<sup>1</sup>Sorbonne Universite and Institut Jean le Rond d'Alembert, CNRS UMR-7190, F57005 Paris, France  
mandeep.saini@sorbonne-universite.fr

<sup>2</sup>Institut Universitaire de France, F57005 Paris, France

In this work, we present numerical simulations of the response of a bubble when the system pressure is suddenly decreased by given amount  $\Delta p$  using numerical method described by Fuster and Popinet<sup>1</sup>. This academic problem is related to the nucleation of cavitation bubbles which occur when small nuclei (air pockets) become unstable and grow explosively. The quasi-static theory is shown to well predict the region of stability for spherical cap nuclei attached to rigid wall in “Ca-Oh” plane (see figure 1), where  $Ca = \frac{\mu_l U_c}{\sigma}$  is capillary number,  $Oh = \frac{\mu_l}{\sqrt{\rho_l \sigma R_{c,0}}}$  is Ohnesorge number,  $\mu_l, \rho_l$ , are the viscosity and density of liquid phase respectively,  $\sigma$  is the surface tension,  $R_{c,0}$  is the initial radius of curvature of the bubble and  $U_c = \sqrt{\frac{2 \Delta p}{3 \rho_l}}$  is the characteristic velocity of problem which can also be obtained by the Rayleigh-Plesset model at zero acceleration. Figure 1b shows that when the bubble is unstable, the temporal evolution of the equivalent bubble radius (e.g. proportional to the cube root of the bubble volume), is shown to reach constant asymptotic velocity ( $U_c$ ), thus, at large scale the motion of bubble interface is given by the inertial effects and visco-capillary effects are negligible.

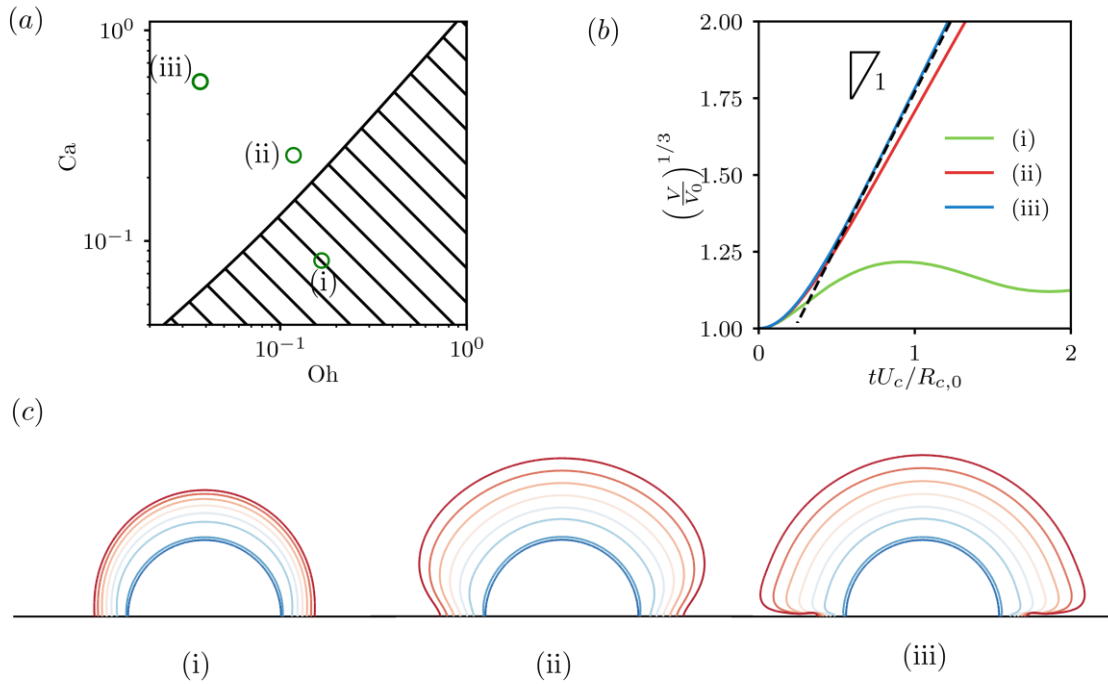


Figure 1: (a) The stability diagram of the cavitation bubbles in Oh-Ca plane, the location of three representative points i - (Oh = 0.17, Ca=0.08), ii - (Oh = 0.11, Ca = 0.26) and iii - (Oh = 0.03, Ca = 0.57). The stable region predicted from quasi-static theory for contact angle of 90 degrees and free slip boundary condition is shaded with hatch lines. (b) The evolution of the equivalent radius three representative cases is shown as obtained from DNS. (c) The evolution of bubble shapes is shown for the three representative cases where the color map corresponds to different non-dimensional simulation times.

The dynamics inside the boundary layer are controlled by visco-capillary effects which, in some conditions, leads to formation of microlayer (micron scale liquid film in case (iii) of figure 1c). The problem is identical to the formation of thin liquid film on solid surfaces, known as the Landau-Levich-Derjaguin-Bretherton (LLDB) problem. Numerical simulations reveal that the microlayer formation is inhibited at small capillary numbers and promoted at large capillary numbers (see case iii of figure 1). A simple model based on Cox-Voinov law for microlayer formation is shown to correctly explain the dependence of capillary numbers beyond which microlayer forms on the microscopic contact angle. We also analyze the height of the microlayer formation which scales with the Reynolds numbers,  $Re = \frac{\rho_l U_c R_{c,0}}{\mu_l}$  and obeys the  $r^{\frac{1}{2}}$  law where  $r$  is the dimensionless distance from the initial location of the contact line as predicted by Guion et. al.<sup>2</sup>. These results for hydrodynamics of microlayer formation are equally valid for the case of boiling where it is known that at short times after nucleation the bubbles grow explosively under the inertial effects.

#### REFERENCES

- [1] Fuster, D., & Popinet, S. (2018). An all-Mach method for the simulation of bubble dynamics problems in the presence of surface tension. *Journal of Computational Physics*, 374, 752-768.
- [2] Guion, A., Afkhami, S., Zaleski, S., & Buongiorno, J. (2018). Simulations of microlayer formation in nucleate boiling. *International Journal of Heat and Mass Transfer*, 127, 1271-1284.

# Light-induced interface instability: optical Taylor cones/jets & breakup

Antoine Girot, Raphaël Saiseau, Julien Petit, Hamza Chraïbi, Thomas Guérin, Ulysse Delabre and Jean-

Pierre Delville

*Univ. Bordeaux, CNRS, LOMA, UMR 5798, Talence F-33400, France, jean-pierre.delville@u-bordeaux.fr*

In a seminal work, Ashkin demonstrated in 1976 [1] that the optical radiation pressure of a laser wave is able to deform a liquid interface (Fig 1a). This effect was further extended to the optical deformation of soft spherical interfaces, aiming at characterizing their rheology [2, 3]. Moreover, if the radiation pressure becomes larger than the Laplace pressure (neglecting buoyancy), then the liquid interface deformation becomes unstable and triggers the formation of a beam-centered liquid jet [4, 5] characterized by a conical shape at the foot of the jet (Fig 1b). If the radiation pressure is still increased, these jets increase in length, to eventually form a liquid column of very large aspect ratio between the interface at rest and the bottom substrate [6]. Such an optical approach thus offers an appealing tool for investigating the formation of optical analogues of Taylor cones/jets (Fig. 1b) and the Rayleigh-Plateau instability either from the drop dripping in presence of optical forcing (Fig. 1c) or in the ‘academic’ situation of a stationary liquid column when shutting down the laser (Fig. 1d). In order to propose a universal thermodynamic point of view, we performed these three types of experiments using a near-critical phase-separated liquid mixture and approaching the critical point. This two-phase system allows to vary both the radiation pressure (through the variation of the refractive index contrast between the two liquid phases) and the Laplace pressure (through the vanishing behavior of the interfacial tension close to criticality). Results will be discussed within the frame of fluctuating hydrodynamics where thermodynamics and fluid dynamics start to be entangled.

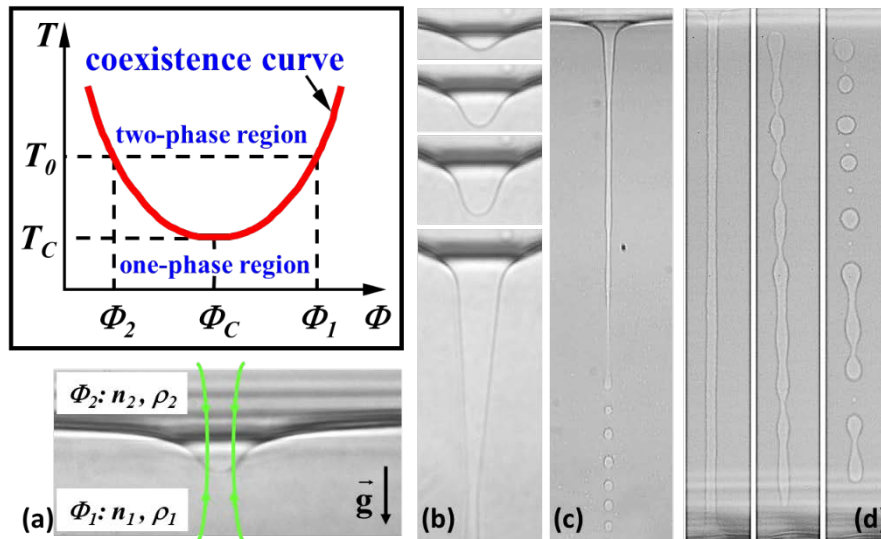


Figure 1: (a) Schematic view of a phase diagram of a near-critical liquid mixture and near-critical interface deformation induced by the radiation pressure of a laser wave (green arrows). (b) Increasing interface deformation and focus on the formation of an optical analogue of a Taylor cone. (c) Whole view of the jetting (cone, ligament and drop dripping). (d) Formation of a liquid column and Rayleigh-Plateau instability when the laser is shut down.

- 
- [1] Ashkin, A., & Dziedzic, J. M. (1973). Radiation pressure on a free liquid surface. *Physical Review Letters*, 30(4), 139.
- [2] Guck, J., Ananthakrishnan, R., Moon, T. J., Cunningham, C. C., & Käs, J. (2000). Optical deformability of soft biological dielectrics. *Physical Review Letters*, 84(23), 5451.
- [3] Delabre, U., Feld, K., Crespo, E., Whyte, G., Sykes, C., Seifert, U., & Guck, J. (2015). Deformation of phospholipid vesicles in an optical stretcher. *Soft matter*, 11(30), 6075-6088.
- [4] Wunenburger, R., Casner, A., & Delville, J. P. (2006). Light-induced deformation and instability of a liquid interface. I. Statics. *Physical Review E*, 73(3), 036314.
- [5] Girot, A., Petit, J., Saiseau, R., Guérin, T., Chraïbi, H., Delabre, U., & Delville, J. P. (2019). Conical interfaces between two immiscible fluids induced by an optical laser beam. *Physical review letters*, 122(17), 174501.
- [6] Petit, J., Rivière, D., Kellay, H., & Delville, J. P. (2012). Break-up dynamics of fluctuating liquid threads. *Proceedings of the National Academy of Sciences*, 109(45), 18327-18331.

# Asymmetric streaming induced by large amplitude vibrations near a sharp obstacle

Geyu Zhong <sup>a,b,c</sup>, Yingwen Liu <sup>c</sup>, Xiaofeng Guo <sup>b</sup>, Laurent Royon <sup>b</sup>, Philippe Brunet <sup>a</sup>,

<sup>a</sup> Laboratoire Matière et Systèmes Complexes (MSC), UMR CNRS 7057, Université Paris Cité, Paris, France

<sup>b</sup> Laboratoire Interdisciplinaire des Energies de Demain (LIED), UMR CNRS 8236, Université Paris, Paris, France

<sup>c</sup> Key Laboratory of Thermo-Fluid Science and Engineering of MOE, Xi'an Jiaotong University, China

Acoustic waves can generate steady streaming within a fluid owing to the generation of viscous boundary layers near walls, of typical thickness  $\delta$ . In microchannels, the acoustic wavelength  $\lambda$  is adjusted to twice the channel width  $w$  to ensure a resonance condition, which implies the use of MHz transducers (given the speed of sound in water 1500 m/s). Recently though, intense acoustic streaming was generated by acoustic waves of a few kHz (hence with  $\lambda \ll w$ ), owing to the presence of sharp-tipped structures of curvature radius at the tip  $r_c$  smaller than  $\delta$ . This enhancement of streaming is due to centrifugal effects that lead to the generation of an intense jet from the sharp tip [1, 2, 3].

Experimentally, this flow has been shown to provide efficient active mixing in microchannels, due to strong transverse velocity, especially when optimizing the space between several of these sharp tips along the channel [4]. The forcing is often prescribed by acoustic transducers, but it can also be generated by low-frequency time-periodic flow ensured by mechanical vibrations.

We quantitatively investigate this sharp-edge acoustic streaming via the direct resolution of the full Navier-Stokes equation, using Finite Element Method. The influence of  $\delta$ ,  $r_c$  and viscosity  $\nu$  on the acoustic streaming performance are quantified. Our results suggest choices of operating conditions and geometrical parameters, in particular the dimensionless tip radius of curvature  $r_c/\delta$  and the liquid viscosity [3].

In a more recent study [5], we investigate the flow structure generated by low-frequency forcing (typically 10 Hz) around a sharp tip. Using Direct Numerical Simulations, we extract both the time-periodic and steady flows within a large span of amplitude of vibrations. When the amplitude is smaller than the tip radius of curvature, we recover the flow structure observed at higher frequencies ( $> 1$  kHz) in previous studies, namely an intense symmetric central jet and a quadratic dependence for the characteristic streaming velocity with the oscillating velocity  $v_s \sim v_a^2$ . At higher amplitudes, such a scaling no longer holds and the streaming flow pattern loses its left-right symmetry. We then analyse the mechanisms of the instability from the careful examination of the instationary flow fields, and we propose possible mechanisms for such a flow transition involving the coupling between the streaming jet and instationary vorticity [5].

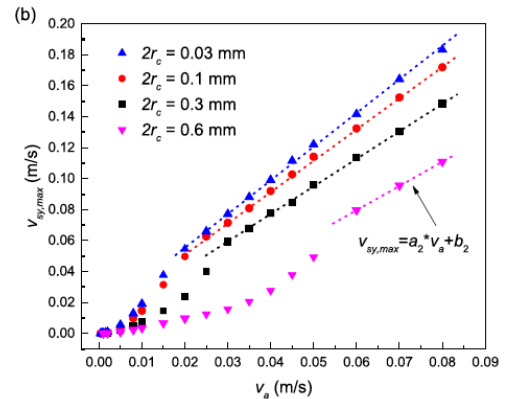
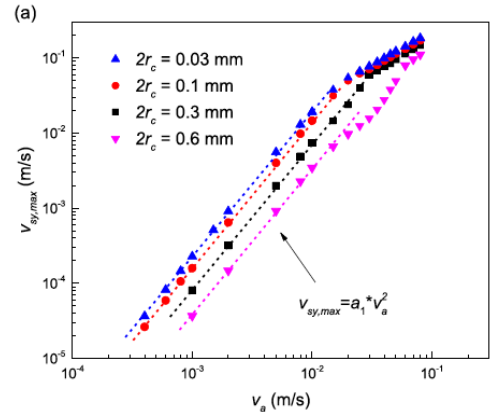
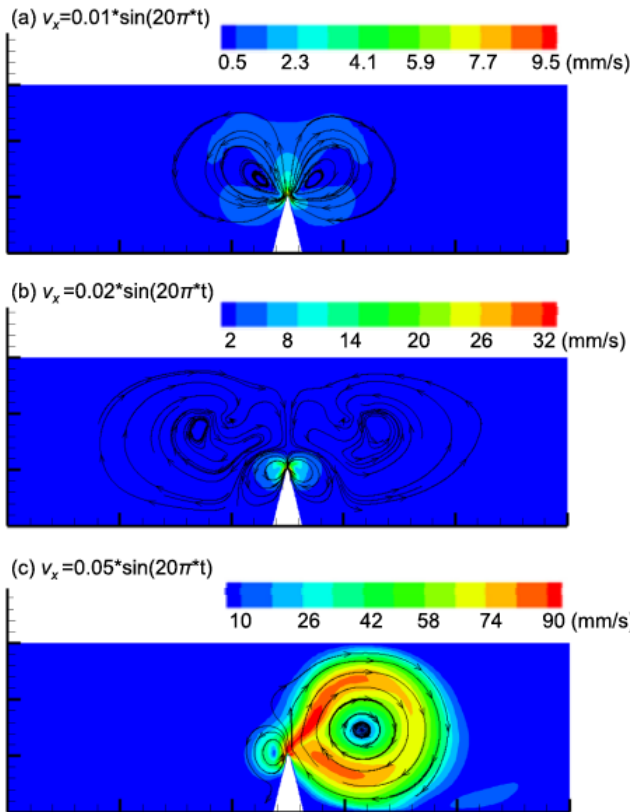


*Figure 1 : (Left) Streaming flow pattern around a sharp structure at various forcing acoustic velocity  $V_x$ . (Right) Maximal streaming velocity versus acoustic velocity amplitude  $V_a$  in Log-Log axes (a) and Lin-Lin axes (b), evidencing the crossover between a quadratic relationship at low  $V_a$  and a linear one at high  $V_a$ .*

#### References:

- [1] M. Ovchinnikov, J. Zhou, and S. Yalamanchili, Acoustic streaming of a sharp edge, *J. Acoust. Soc. Am.* 136, 22 (2014).
- [2] C. Zhang, X. Guo, P. Brunet, M. Costalonga, and L. Royon, Acoustic streaming near a sharp structure and its mixing performance characterization, *Microfluid. Nanofluid.* 23, 104 (2019).
- [3] C. Zhang, X. Guo, L. Royon, and P. Brunet, Unveiling of the mechanisms of acoustic streaming induced by sharp edges, *Phys. Rev. E* 102, 043110 (2020).
- [4] C. Zhang, P. Brunet, L. Royon, and X. Guo, Mixing intensification using sound-driven micromixer with sharp edges, *Chem. Eng. J.* 410, 128252 (2021).
- [5] G. Zhong, Y. Liu, X. Guo, L. Royon and P. Brunet. Vibration-induced streaming flow near a sharp edge: Flow structure and instabilities in a large span of forcing amplitude. *Physical Review E* 107, 025102 (2023).

---

# Red Blood Cell Dependent Calcium Dynamics from Endothelial Cells

Ananta Kumar Nayak<sup>\*1</sup>, Sovan Lal Das<sup>2</sup>, and Chaouqi Misbah<sup>3</sup>

<sup>1</sup>Univ. Grenoble Alpes – University of Grenoble Alpes, CNRS, LIPhy, F-38000 Grenoble, France – France

<sup>2</sup>IIT Palakkad – India

<sup>3</sup>Univ. Grenoble Alpes – University of Grenoble Alpes, CNRS, LIPhy, F-38000 Grenoble, France – France

## Abstract

Red blood cells (RBCs) are known to release adenosine triphosphate (ATP), a signaling molecule in presence of flow. ATP molecules then bind to purinergic receptors (P2Y2) on the plasma membrane of endothelial cells (ECs), to activate a cascade of biochemical reactions. Further, this triggers the release of ubiquitous calcium ions from endoplasmic reticulum (ER). As a result, the cytoplasmic calcium concentration rapidly increases from its physiological concentration ( $0.1 \mu\text{M}$ ) to a few  $\mu\text{M}$  concentration. Calcium is well known to regulate the activity of many enzymes in order to perform cellular functioning. However, the presence of high cytoplasmic calcium concentration for longer time causes the formation of calcium phosphate, which eventually leads to pathological conditions like death of cell. In order to avoid such consequences, EC manages to maintain its physiological calcium concentration in presence of ATP using ATP-driven pumps present in plasma/ER membrane and the desensitization of P2Y2 receptors. Thus, the intracellular calcium homeostasis is maintained within an EC. In order to emulate these experimental facts, we proposed a homeostatic calcium dynamics model by considering the receptor dynamics. In that model, we use a constant ATP concentration without apriori knowing neither the source of ATP concentration nor the variation of concentration from EC to EC in the vascular bed. In vasculature, ATP released by RBCs and ECs and hydrolysis of ATP by ectonucleotidase enzymes, present on the EC membrane, can alter and stabilize the concentration of ATP. As a result, the concentration of calcium will vary from EC to EC, which may affect vascular homeostasis. In order to study that, we couple the EC calcium to RBC flow in a two-dimensional channel for a given imposed parabolic flow. We conducted several simulations by varying flow strength, channel width, and concentrations of RBC (hematocrit), in order to emulate the blood flow in microcirculation. We found that the endothelium helps in maintaining a steady ATP concentration, avoiding the abnormal rise in the ATP concentration released from RBCs. With varying flow strength and hematocrit for a given channel width, we found that the ATP concentration and the cytoplasmic transient concentration increase with increase in the flow strength and hematocrit, and this leads to the cytoplasmic calcium transient time decrease. Due to the relatively smaller peak times and higher amplitudes of cytoplasmic calcium at high flow strength as compared to that at low flow strength for all hematocrit, there is a possibility of calcium propagation from the high flow strength region to the low flow strength region for the coordination of cellular functions. Similarly, we observed a possibility of calcium propagation from low confined channels to the medium or highly confined channels for all hematocrit at a given flow strength.

---

\*Speaker

---

# CONFINEMENT-TRIGGERED NON-TRIVIAL DYNAMICS OF RED BLOOD CELLS UNDER CONJUGATE INTERPLAY OF ELECTRIC FIELD AND POISEUILLE FLOW

Somnath Santra<sup>\*1</sup>, Alexander Farutin<sup>2</sup>, and Chaouqi Misbah<sup>3</sup>

<sup>1</sup>Postdoctoral Researcher – Universite Grenoble Alpes, CNRS, LIPhy, 38000 Grenoble – France

<sup>2</sup>Laboratoire Interdisciplinaire de Physique – Universite Grenoble Alpes, CNRS, LIPhy, 38000 Grenoble – France

<sup>3</sup>Laboratoire Interdisciplinaire de Physique – Universite Grenoble Alpes, CNRS, 38000 Grenoble, chaouqi.misbah@univ-grenoble-alpes.fr – France

## Abstract

Migration of Red blood cells (RBCs) in microchannels is a phenomenon ubiquitous in the microvascular networks of the human body consisting of several small microvessels like arterioles, capillaries, and venules. One enthralling aspect is that the RBC membrane is non-neutral due to the presence of the negatively charged lipid head groups embedded inside the membrane under normal physiological conditions. Therefore, the dynamics can be altered at will by applying an electric field in physiological ranges ( $\leq 100$  mVmm<sup>-1</sup>). With the emergence of Biomedical Microelectromechanical (BioMEMS) technology, the non-neutral nature of RBCs membrane is exploited in vitro in lab-on-a-chip devices, flow cytometry, cell separation, and CAR T-cell therapy, just to name a few for the on-chip diagnosis of pathological states and abnormalities(1). In these biomedical applications, the geometry-driven confinement effect is omnipresent. In the present study, we have experimentally investigated the channel confinement-induced spatial dynamics of RBCs under conjugate interplay of electric field and Poiseuille flow. It is worth mentioning that although bulk changes in red blood cell concentration between microvessels are well studied and reported, local distributions under electrical forces are completely overlooked. In presence of an electric field, RBCs aggregate, deform, and migrate within microvessels, forming heterogeneous distributions which have significant effects on local hemodynamics and may dictate several pathological states. To perform experiments, we fabricated a PDMS-based compact microfluidic chip with embedded electrodes at the inlets and outlets of the channel. Channel's height and length are made as 6  $\mu\text{m}$  and 4.2 cm, respectively. We have taken the channel widths of 50  $\mu\text{m}$  and 30  $\mu\text{m}$ , to infer the channel confinement as weak and tight. The device is placed on an inverted microscope (IX70, Olympus) attached to a high-speed camera (Fastcam Mini, Photron), and an X60 objective. Before, passing the sample (an emulsion of phosphate buffer saline and RBCs), the microchannels are passivated with BSA (bovine serum albumin, Sigma) solutions. A DC electric field is applied along the channel in the direction of flow, supplied from a DC source meter by the electrodes. To control the pressure drop between the inlet and outlet and maintain the circulation of solutions in the microfluidic channel, a pressure controller

---

\*Speaker

(Elveflow) has been employed. In microflows, RBCs self-organize in the flow direction by stacking very closely and thus buildup linear clusters of different lengths. The most stable and linear structures are called trains. The present study shows that at moderately high hematocrit ( $\approx 8\%$ ), longer trains are formed and they are aligned in the direction of flow when there is no imposed electric field. However, the presence of an electric field surprisingly shifts the distribution down to shorter values thus leading to a smaller average train length. In addition, in the tightly confined domain, the average orientation angle of RBC trains increases with the increase in the applied voltage, whereas in weakly confined domain, the average orientation angle of RBC trains decreases monotonically with the increase in the applied voltage. Another interesting finding is that in a tightly confined domain, RBCs are more focused toward the centerline in presence of an electric field whereas, in the weakly confined domain, alternating bands of high and low RBC concentration in the cross-flow direction become more pronounced when an electric field of physiological strength is applied. Confinement-triggered electro-kinetic motion and its reversal depending on the degree of confinement is responsible for these phenomena. In brief, in the tightly confined domain, not only the electroosmotic force tends to move the RBCs toward the flow direction but also tends to organize the RBCs towards the centerline. On the other hand, the electrophoretic force tends to move it in the opposite direction in the weakly confined domain. We have also experimentally found that the electric field-induced velocity of RBCs in the confined channel is higher as compared to the weakly confined domain. These findings are anticipated to shed new light on the possibility of manipulating RBC dynamics in constrained microenvironments, with significant implications for medical research and technology development.

**Keywords:** RBCs, electric field, average train length, average orientation angle, weakly and tightly confined domain.

#### References

- (1) Kinosita K Jr, Tsong TT. Hemolysis of human erythrocytes by transient electric field. Proc Natl Acad Sci U S A;74(5):1923-7, 1977

# Microscale liquid flow driven by the capillary interaction with an isolated micro-particle

Harunori N. Yoshikawa,<sup>1</sup> Georg Dietze<sup>2</sup>, Farzam Zoueshtiagh<sup>3</sup>, Lizhong Mu<sup>4</sup> and Ichiro Ueno<sup>5</sup>

<sup>1</sup> Université Côte d'Azur, CNRS, Institut de Physique de Nice, 06100 Nice, France harunori@unice.fr

<sup>2</sup> Université Paris-Saclay, CNRS, FAST, 91405, Orsay, France

<sup>3</sup> Univ. Lille, CNRS, Centrale Lille, Univ. Polytechnique Hauts-de-France, UMR 8520, IEMN, F59000 Lille, France

<sup>4</sup> Key Laboratory of Ocean Energy Utilization and Energy Conservation of Ministry of Education, School of Energy and Power Engineering, Dalian University of Technology, China

<sup>5</sup> Division of Mechanical Engineering, School of Science and Technology, Tokyo University of Science, Chiba 278-8510, Japan

Capillarity often plays a significant role in the flow dynamics of systems with immiscible fluid-fluid interfaces. This tendency is reinforced in microscale fluid systems where interfaces are often curved significantly due to narrow flow passages and/or to the formation of three-phase contact lines on multiple adjacent walls. We investigate a flow in a thin liquid film on a fully wettable substrate with an isolated particle (Fig. 1a) at the initial stage of the flow-particle dynamical interaction. The film advances on the substrate due to the substrate high wettability. The film thickness and the particle diameter are both of the order of 1 to 10  $\mu\text{m}$ . The contact of the film advancing front with the particle leads to the formation of a meniscus around the particle. The growth of the meniscus is accompanied by a quick local transport of liquid along the direction perpendicular to the liquid advancing front (Fig. 1b). Performing theoretical modeling and numerical simulations, we show that this abrupt acceleration results from a negative pressure of the meniscus due to capillarity [1, 2]. The numerical simulation also discloses complex instantaneous flow structures: entangled streamlines showing a horseshoe-like vortex [3]. Detailed analysis of the pressure field variation in the meniscus reveals that the vortex is generated by the adverse pressure gradient due to the capillarity.

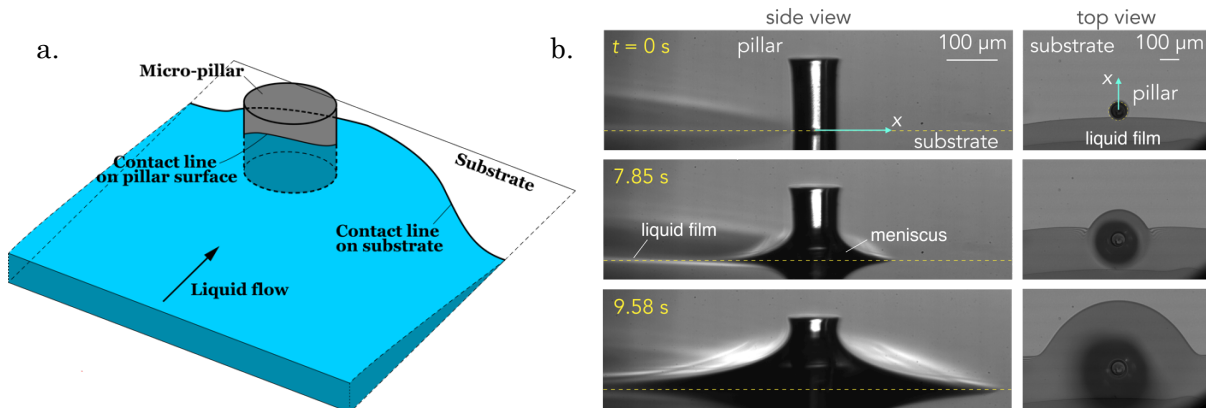


FIG. 1. Microscale fluid system. (a) Schematic illustration of a liquid film advancing on a substrate in the presence of a micro-pillar. (b) The initial stage of the flow-particle interaction observed in an experiment.

- [1] L. Mu, D. Kondo, M. Inoue, T. Kaneko, H.N. Yoshikawa, F. Zoueshtiagh and I. Ueno, Sharp acceleration of a macroscopic contact line induced by a particle, *J. Fluid Mech.* **830**, R1 (2017).  
 [2] H. Nakamura, V. Delafosse, G. F. Dietze, H. N. Yoshikawa, F. Zoueshtiagh, L. Mu, T. Tsukahara and I. Ueno, Enhancement of meniscus pump by multiple particles, *Langmuir*, **36**(16), 4447-4453 (2020).  
 [3] K. Ozawa, H. Nakamura, K. Shimamura, G. F. Dietze, H. N. Yoshikawa, F. Zoueshtiagh, K. Kurose, L. Mu, I. Ueno, Capillary-driven horseshoe vortex forming around a micro-pillar, *J. Colloid Interface Sci.* **642**, 227-234 (2023).

# Light-responsive liquid-liquid phase separation in microfluidic droplets

Nicolas Martin<sup>1</sup>, Zi Lin<sup>1</sup>, Thomas Beneyton<sup>1</sup> and Jean-Christophe Baret<sup>1</sup>

<sup>1</sup> Centre de Recherche Paul Pascal, Univ. Bordeaux-CNRS, UMR5031, 33600 Pessac, France  
nicolas.martin@crpp.cnrs.fr

Liquid-liquid phase separation (LLPS) is a ubiquitous phenomenon in extant biology. Living cells exploit biomolecular condensates produced by LLPS to organize their contents. These membrane-less organelles dynamically form and dissolve in response to environmental cues, which allows cells to orchestrate biochemical processes. Coacervate droplets formed via LLPS of oppositely charged polyions have emerged in recent years as promising models of biomolecular condensates.[1] It is yet still very challenging to precisely control in space and time the formation and dissolution of coacervate droplets *in vitro*. To overcome this limitation, we have recently designed photoswitchable coacervates that reversibly form and dissolve in response to light, offering excellent spatiotemporal control over LLPS.[2] These coacervates are produced by complexation between oligonucleotides and azobenzene cations (FIG. 1A), which reversible trans-cis photoisomerisation regulates the formation and dissolution of coacervate droplets. To gain deeper insight into this light-actuated LLPS phenomenon, we here exploit droplet-based microfluidics to produce physically isolated coacervate droplets with a well-defined composition and environment [3] (FIG. 1B). This approach allows us to precisely monitor the kinetics of light-induced coacervate dissolution and reformation, and extract characteristic scaling laws that we can compare to azobenzene isomerisation, diffusion and nucleation/growth processes [4] (FIG. 1C). Altogether, droplet-based microfluidics provides a robust approach to decipher the mechanism of light-actuated liquid-liquid phase separation, which opens perspectives to dynamically control the localization and reactivity of biomolecules.

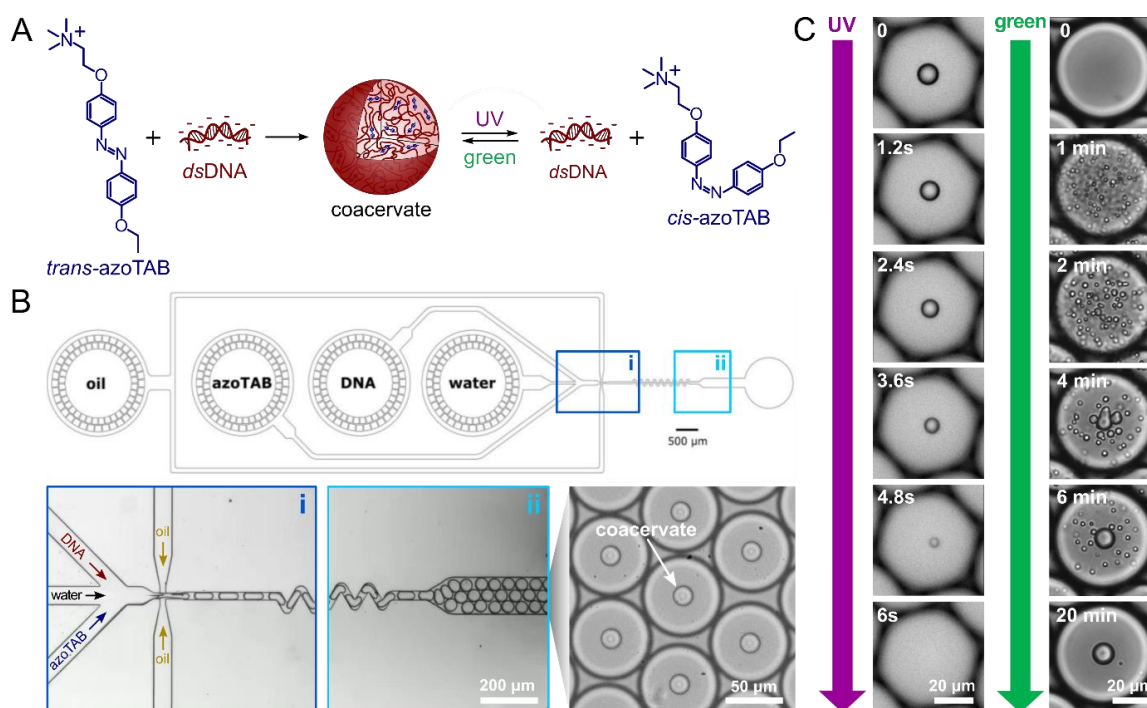


FIG. 1. A: Scheme of light-switchable coacervation between azobenzene cations and double stranded DNA; B: Production of monodisperse coacervate droplets via droplet-based microfluidics; C: Time-lapse optical microscopy images of UV- and green light-mediated coacervate dissolution and formation, respectively, in a single microfluidic emulsion droplet.

- [1] N. Martin, Dynamic synthetic cells based on liquid-liquid phase separation, *ChemBioChem* **20**, 2553 – 2568 (2019)  
[2] N. Martin, L. Tian, D. Spencer, A. Coutable-Pennarun, J. L. R. Anderson, S. Mann, Photoswitchable phase separation and oligonucleotide trafficking in DNA coacervate microdroplets, *Angew. Chem. Int. Ed.* **58**, 14594 – 14598 (2019)  
[3] T. Beneyton, C. Love, M. Girault, T.-Y. D. Tang, J.-C. Baret, High-throughput synthesis and screening of functional coacervates using microfluidics, *ChemSystemsChem* **2**, e2000022 (2020)  
[4] Z. Lin, S. Lafon, T. Beneyton, X. Brilland, L. Buisson, A. Baron, J.-C. Baret, N. Martin, *In preparation*

# Mechano-Physical Responsiveness of Deformable Microchannels – How the Flow Medium Matters

Suman Chakraborty and Sampad Laha

Department of Mechanical Engineering, Indian Institute of Technology Kharagpur, Kharagpur-721302,

India

E-mail: [suman@mech.iitkgp.ac.in](mailto:suman@mech.iitkgp.ac.in)

## Abstract

Flow through deformable microchannels has been attracting significant research attention in recent times, owing to the underlying rich physics of complex fluid structure interaction on one hand and its exciting biomimetic applications, on the other hand, spanning across the realms of physiology of health and diseases, disease detection and targeted therapy for its effective management. Here we bring out the contrasting hydrodynamic features of non-biological, biologically passive and active suspensions of aqueous media flowing through a deformable microfluidic conduit, with particular focus on unravelling the micro-scale hemodynamics of cellular suspensions. We exemplify our illustration via experimentations on biomimetic flexible polydimethylsiloxane microfluidic channels made of sylgard materials of varying base to crosslinker ratios. The microchannel deformation dynamics is characterised using inverted microscopy and high speed imaging. Xanthan gum solutions (established synthetic blood analogue) of different concentrations are first deployed to analyse different levels of shear thinning characteristics, resulting in distinctive deformation and flow behaviour, coupled by a nonlinear axial variation in the pressure field as a specific signature of the fluid-structure interactions over small scales. Further, in order to bring out the implications of active cellular matter in hemodynamic transport, the transport of red blood cell suspensions of varying hematocrit levels is elucidated, deciphering contrasting characteristics as compared their inert rheological analogues. Our results reveal discernible attenuation of the channel deformation on account of the presence of enriched cellular entities. By virtue of being non-trivially connected with the shear-thinning rheology of blood, our study opens up several important questions at the interface of suspension rheology and flexible microfluidics, especially in context of bio microfluidics applications, centrally connected with the dilemma of the differential dynamic responses of active versus passive fluidic media under an otherwise similar mechano-physical framework.

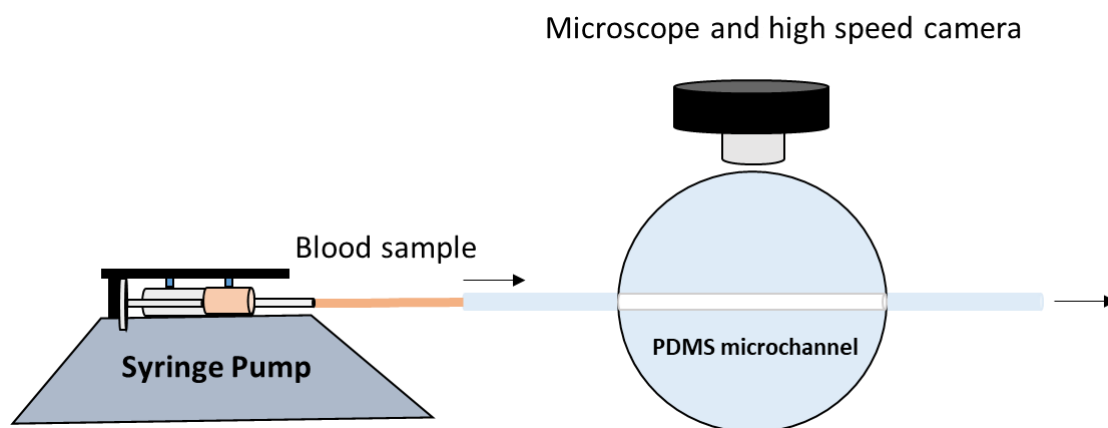


**Fig. 1** The experimental setup schematic

---

# Experimental Investigation of Bubble Rising Through Liquid-Liquid Interface in Presence and Absence of Surfactant

Bahni Ray\*<sup>1</sup> and Rabbani Ghulam\*<sup>1</sup>

<sup>1</sup>Indian Institute of Technology Delhi – India

## Abstract

The bubble rising through gas-liquid interface has been widely studied due to its relevance in various industrial processes and environmental phenomena<sup>1</sup>. The presence of surfactant in the liquid phase can alter the dynamics of bubble rising and lead to bubble rupture<sup>2</sup>. We conduct experiments using a transparent acrylic container filled with water and introduce a single gas bubble into it. The trajectory and shapes of bubble in absence of surfactant is shown in FIG.1 and FIG.2. We investigate the influence of surfactant (cetyltrimethylammonium bromide<sup>3</sup>) in water on the bubble dynamics, including the bubble shape, size and rise velocity. The surfactant molecules adsorb at the bubble interface, leading to the formation of a surfactant-laden film around the bubble. This film can affect the bubble shape and size. This can also influence the occurrence of bubble rupture during the rising process. The behaviour of bubbles at the interface is also investigated, and it is observed that the bursting of the bubbles at the interface could be earlier in presence of surfactant. This indicates the bubble stability and weakening of the bubble surface at the interface leading to early bursting. Overall, this study provides valuable insights into the dynamics of bubble rising and bursting in presence and absence of surfactant.

---

\*Speaker

---

# Viscocapillary Lift Force at the Fluid Interface

Aditya Jha\*<sup>1</sup>, Yacine Amarouchene<sup>2</sup>, and Thomas Salez<sup>2</sup>

<sup>1</sup>Laboratoire Ondes et Matière d'Aquitaine – Centre National de la Recherche Scientifique : UMR5798, Université de Bordeaux : UMR5798, Université de Bordeaux, Centre National de la Recherche Scientifique – France

<sup>2</sup>Laboratoire Ondes et Matière d'Aquitaine – Centre National de la Recherche Scientifique : UMR5798, Université de Bordeaux : UMR5798, Université de Bordeaux, Centre National de la Recherche Scientifique – France

## Abstract

The force exerted on an object moving in a viscous fluid, and its modification induced by the presence of a nearby boundary, have been abundantly studied in fluid mechanics for the past century. In the last decades, soft gels and elastomers<sup>(1)(2)(3)</sup> have been of growing interest, and have been shown to break the symmetry of nearby low-Reynolds-number flows, thus generating a force normal to the substrate. Such a lift force depends in particular on the material properties of the substrate and the intervening fluid. Here, we revisit this problem, by addressing the novel situation where the soft substrate is replaced by a fluid interface. We analyze in details the lubrication flow between a moving object and the interface. Using a combination of analytical and numerical treatments, we derive an expression of the viscocapillary lift force at leading order in compliance.

1J. Skotheim and L. Mahadevan, *Phys. Rev. Lett.* **92.24**, 245509 (2004).

2V. Bertin *et al.*, *Journal of Fluid Mechanics* **933** (2022).

3A. Kargar-Estahbanati and B. Rallabandi . *Phys. Rev. Fluids* **6.3**, 0.34033 (2021)

---

\*Speaker

# Hydrodynamic dispersion in porous media enhances reaction in spherical fronts

Pratyaksh Karan<sup>1,a</sup>, Uddipta Ghosh<sup>2,b</sup>, Yves Méheust<sup>1,c</sup> and Tanguy Le Borgne<sup>1,d</sup>

<sup>1</sup>Geosciences Rennes, UMR 6118, CNRS, Université de Rennes 1, Rennes, 35042, France

<sup>2</sup>Department of Mechanical Engineering, IIT Gandhinagar, 382055, Gujarat, India

<sup>a</sup>[pratyakshkaran@gmail.com](mailto:pratyakshkaran@gmail.com) <sup>b</sup>[uddipta.ghosh@iitgn.ac.in](mailto:uddipta.ghosh@iitgn.ac.in)

<sup>c</sup>[yves.meheust@univ-rennes1.fr](mailto:yves.meheust@univ-rennes1.fr) <sup>d</sup>[tanguy.le-borgne@univ-rennes1.fr](mailto:tanguy.le-borgne@univ-rennes1.fr)

Reaction fronts, characterized as the region in which two miscible fluids, one of which displaces the other one, react with each other, are typically sustained by fluid mixing and play a central role in a large range of porous media systems and applications [1,2]. Some examples include the transport of chemotactic agents in tumour microenvironments [3] and the spreading of injected drugs in human and animal tissues. In many cases, point-wise continuous injection of a reactant that displaces a resident reactant in three dimensions leads to a growing spherical reaction front. While such configurations have until now been studied under the assumption of a constant diffusion coefficient, in porous media the dominant diffusive process at the continuum scale is hydrodynamic dispersion, which depends linearly on the flow velocity.

Hydrodynamic dispersion is the Darcy scale manifestation of the interaction between molecular diffusion and advection by the heterogeneous pore scale velocity field. The Dispersion coefficient is expressed by a second rank tensor that is customarily taken to be a linear function of the local discharge rate [4,5]. In most practical cases, it dominates pure molecular diffusion by several orders of magnitude. Due to its dependence on the local Darcy velocity, hydrodynamic dispersion may strongly influence the dynamics of reactive fronts, and thus significantly alter the local and global reaction rates. However, its effect on spherical reaction fronts is so far unknown.

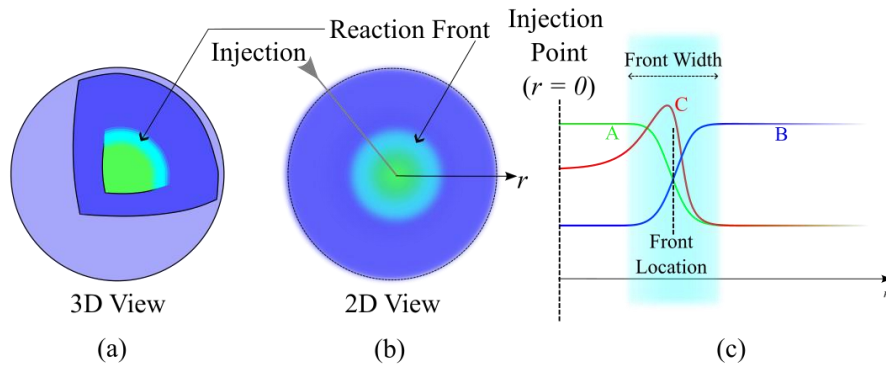


FIG. 1. Illustrative representations of the spherical reaction front; the plot cartoon in panel c demonstrates a typical reaction front and the typical radial concentration profiles for the reactants (A and B) and the product (C) in the front's vicinity.

Here, we analyze the impact of this non-uniform and time-varying hydrodynamic dispersion on reactive transport occurring in such a spherically-advected reaction front under point injection and at constant flow rate. This physical setup is illustrated in Fig. 1. We develop a mathematical framework considering the Advection-Dispersion-Reaction Equation (ADRE) and an irreversible bimolecular  $A+B \rightarrow C$  reaction, the reactant A being continually injected at a point into a porous medium that is initially saturated with the species B. To unveil the essential physics of the impact of hydrodynamic dispersion on the dynamics of the reaction fronts and in order to maintain focus on the exclusive contributions of hydrodynamic dispersion, the medium's permeability is assumed to be uniform. We carry out numerical simulations and derive new asymptotic analytical solutions, which show good agreement with the

- 
- [1] M. Dentz, T. Le Borgne, A. Englert, and B. Bijeljic, Mixing, spreading and reaction in heterogeneous media: A brief review, *J. Contam. Hydrol.* **120**, 1 (2011).  
[2] A. J. Valocchi, D. Bolster, and C. J. Werth, Mixing-limited reactions in porous media, *Transport in Porous Media* **130**, 157 (2019).  
[3] J. Priyadarshani, P. Awasthi, P. Karan, S. Das, and S. Chakraborty, Transport of vascular endothelial growth factor dictates on-chip angiogenesis in tumor microenvironment, *Phys. Fluids* **33**, 031910 (2021).  
[4] L. De Arcangelis, J. Koplik, S. Redner, and D. Wilkinson, Hydrodynamic dispersion in network models of porous media, *Phys. Rev. Lett.* **57**, 996 (1986).  
[5] P. Saffman, A theory of dispersion in a porous medium, *J. Fluid Mech.* **6**, 321 (1959).

numerical results. At early and intermediate times, hydrodynamic dispersion qualitatively alters the transient front properties (front location, width and global reaction rate). During this initial transient regime, dispersion leads to a more advanced reaction front and a larger global reaction rate than when molecular diffusion is the only mixing process apart from advection, as well as to different temporal scalings for the reaction front properties. On the other hand, at sufficiently large times, the reaction front reaches a steady state, characterized by a static position and time-independent reactant concentrations and reaction rate, regardless of the presence and strength of dispersion. When dispersion is weak, the steady state front is positioned in a region where dispersion is negligible compared to diffusion. Conversely, when dispersion is large, the steady state front is positioned in the transition zone where dispersion and diffusion are comparable. In this second scenario, hydrodynamic dispersion permanently affects the reaction front's transport by altering the steady state itself and augmenting the global reaction rate. We establish the quantitative threshold strength of dispersion for this second scenario to exist, which is found to depend on the flow characteristics.

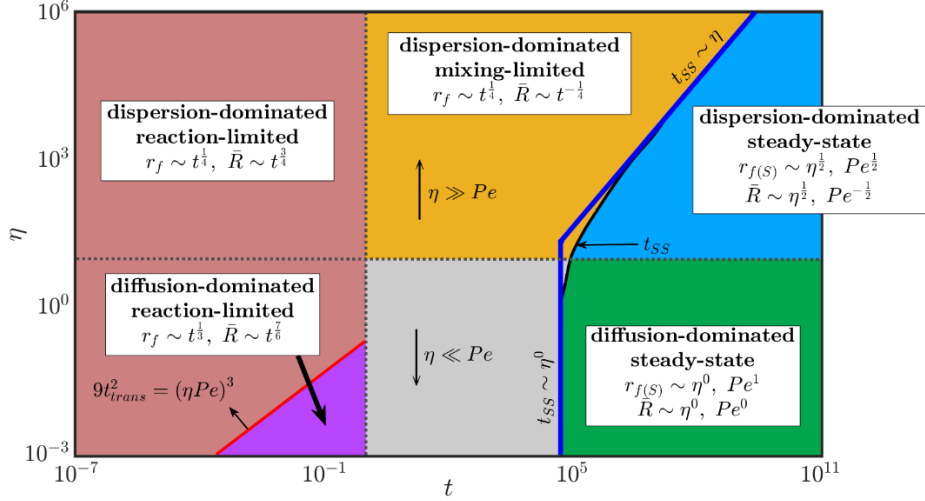


FIG. 1. Phase diagram for the reactive transport regimes of spherically-advected reaction fronts for  $Pe = 10$ , as a function of time and  $\eta$ .

The different regimes that are recovered for a spherical reaction front are summarized in the regime diagram of Fig. 2. The variables  $r_f$  and  $\bar{R}$  represent the front's radial location and the global reaction rate (i.e. the pointwise reaction rate integrated over the entire volume) respectively, whereas  $t$  is time, all three variables being dimensionless (the non-dimensionalization scheme is presented in tab. 1). The parameters  $Pe$  and  $\eta$  represent the Péclet number (corresponding to the typical ratio of the strength of advection to that of molecular diffusion) and the normalized dispersion length. As a consequence, the factor  $\eta Pe$  quantifies the overall strength of dispersion. Evidently, for a strong enough dispersion, apart from the early time front location and reaction rate scaling being different from a dispersion-free scenario, the steady state is reached at a comparatively later time and exhibits a different scaling in terms of  $\eta$  and  $Pe$ , and indeed exhibits a larger magnitude for both the front's radial location and the global reaction rate.

Variable	Characteristic Scale	Remarks
Concentration ( $c_c$ )	$c_0$	Injection concentration of species A (same as ambient concentration of B)
Time ( $t_c$ )	$(k_R c_0)^{-1}$	Reaction time scale
Coordinate length ( $r_c$ )	$(Q_0 / (k_R c_0))^{1/3}$	Volume flow rate is $4\pi Q_0$
Discharge rate ( $q_c$ )	$Q_0 / r_c^2$	
Hydraulic head ( $h_c$ )	$(Q_0 / K)^{2/3} (k_R c_0)^{1/3}$	

TAB. 1. Characteristic scales of relevant variables.

# Droplet growth in warm cumulus clouds

Pijush Patra and Anubhab Roy

Department of Applied Mechanics, Indian Institute of Technology Madras, Chennai 600036, India

The collision of particles sedimenting in a flow field is relevant to many environmental and industrial processes, such as droplet growth in warm clouds and the aggregation of aerosol particles in industrial settings. The evolution of the drop size distribution in clouds depends on the collision rate between the drops, where the combined effects of background flow, gravity, and interparticle interactions drive the collision dynamics. A study of this problem might explain the condensation-coalescence bottleneck (or the ‘size gap’ of 15 - 40  $\mu\text{m}$  droplets) in warm rain formation, where neither condensation nor gravitational collision alone is the dominant growth mechanism [1]. We have focused on studying the collision dynamics of particle pairs subject to a background flow (simple shear flow, turbulent flow) and gravity, incorporating hydrodynamic and interparticle interactions.

In the first problem, we have studied the role of Brownian motion role in the coagulation of bidisperse like-charged spherical particles interacting via non-continuum hydrodynamics, van der Waals, and electrostatic interactions. We have found that electrostatic interactions can enhance the collision rate between like-charged Brownian particles while interacting through non-continuum hydrodynamics, and their charge ratio is high [4]. To consider the effect of a background flow, we have studied the collision of hydrodynamically interacting particle pairs settling in a laminar simple shear flow [3]. By incorporating non-continuum hydrodynamics, van der Waals interactions, and the coupled driving forces of sedimentation and simple shear, our work provides collision efficiency results relevant to flows of suspensions through vertical pipes and channels, sampling of aerosols, and the transport of particulate matter in riser reactors. We have quantified the effects of electrostatic interactions on the collision dynamics of tiny like-charged particles sedimenting through a quiescent gaseous medium [5, 2]. Finally, we have also investigated collision dynamics of sub-Kolmogorov interacting spheres rapidly settling in a homogeneous isotropic turbulent flow. This work relied on formulating an equation for the pair probability PDF and solving it semi-analytically.

## References

- [1] W. W. Grabowski and L.-P. Wang. Growth of cloud droplets in a turbulent environment. *Annual review of fluid mechanics*, 45:293–324, 2013.
- [2] P. Patra, D. L. Koch, and A. Roy. Collision efficiency of like-charged spheres settling in a quiescent environment. *Under revision in Journal of Fluid Mechanics*.
- [3] P. Patra, D. L. Koch, and A. Roy. Collision efficiency of non-brownian spheres in a simple shear flow – the role of non-continuum hydrodynamic interactions. *Journal of Fluid Mechanics*, 950:A18, 2022.
- [4] P. Patra and A. Roy. Brownian coagulation of like-charged aerosol particles. *Physical Review Fluids*, 7(6):064308, 2022.
- [5] N. Thiruvankadam, P. Patra, P. V. Kadaba, and A. Roy. Pair trajectories of uncharged conducting spheres in an electric field. *Physics of Fluids*, 2023.

# Hydrodynamics of Droplet Based Lysozyme Protein Crystal Growth

P K Panigrahi

Department of Mechanical Engineering, IIT Kanpur, UP 208016, India panig@iitk.ac.in

Lysozyme has been used clinically for the treatment of periodontitis, cancer treatment for its analgesic effect and as an agent in antibiotic therapy. Vapor diffusion is the most common method of protein crystallization using either hanging drop or sessile droplet configuration. Several parameters i.e., droplet volume, protein concentration inside the droplet, reservoir volume, number of droplets, and arrangement of droplets influence the yield and quality of protein crystal [1]. The crystal growth process is associated with several multi-physics transport phenomena i.e., evaporation, condensation, and Marangoni flow etc. Therefore, the design of a protein crystallization system depends on clear understanding of the relevant transport processes. The present study reports the detailed transport processes associated with a droplet-based protein crystal growth system.

The micro particle image velocimetry is used to characterize the velocity field inside the droplet [2]. Digital holographic interferometry is used to characterize the vapor cloud outside the evaporating interface [3]. The sessile droplet configuration is used for protein crystal growth (See Figure 1). Fluid convection increases the crystal growth rate due to increase in solute supply to interface. However, strong convective flow can also adversely affect the crystal quality leading to the incorporation of impurities on the crystal surface. Therefore, there have been attempts to reduce the convection strength using micro gravity environment, external magnetic field, and electric field. The present study demonstrates that the use of droplet confinement and geometric arrangement of evaporating interface can influence the evaporation rate and hence crystal quality. The reduction in evaporation rate is attributed to the interaction between vapor cloud between the evaporating interface.

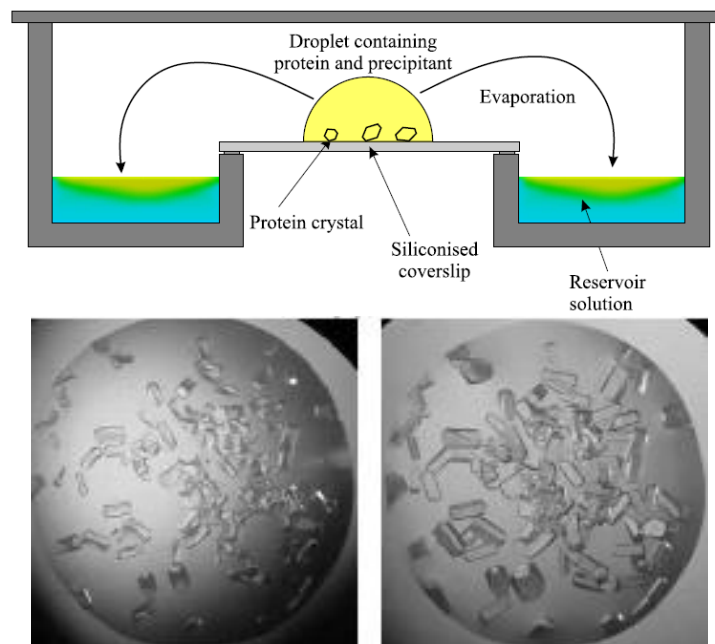


FIG. 1. Top: Schematic of the droplet-based protein crystal growth system; Bottom: Sample image of protein crystal growth inside the droplet at two time instants.

- 
- [1] A. S. Gupta, R. Gupta, P. K. Panigrahi and K. Muralidhar, *Imaging transport phenomena during lysozyme protein crystal growth by the hanging drop technique*, Journal of Crystal Growth 372 19–33 (2013).  
[2] T. K. Pradhan and P. K. Panigrahi, *Suppressing internal convection of a droplet using confinement during protein crystallization*, J. Appl. Phys. 128, 084701 (2020).  
[3] D. Shukla and P K Panigrahi, *Digital Holographic Interferometry Investigation of Liquid Hydrocarbons Vapor Cloud Above a Circular Well*, Applied Optics, Vol 59, No. 19, 5851 (2020).

# Universal spreading dynamics of blood through porous matrix: Effect of cellular aggregation and limited sample volume in the micro-porous domain

Sampad Laha<sup>1</sup>, Shantimoy Kar<sup>2,3</sup> and Suman Chakraborty<sup>1,2</sup>

<sup>1</sup>*Department of Mechanical Engineering, Indian Institute of Technology, Kharagpur, India, [suman@mech.iitkgp.ac.in](mailto:suman@mech.iitkgp.ac.in)*

<sup>2</sup>*Advanced Technology Development Centre, Indian Institute of Technology, Kharagpur, India*

<sup>3</sup>*Department of Medical Devices, National Institute of Pharmaceutical Education and Research (NIPER) Hyderabad, India*

Understanding the complex spreading dynamics of physiological fluids through porous matrix such as paper, holds paramount importance in dictating the functionalities of a wide variety of diagnostic kits that are now-a-days being deployed for rapid detection of diseases harnessing body-fluid based bio-sensing at point-of-care. In contrast to the intuitive paradigm that dynamics of whole blood on paper matrix is likely to be strongly dependent on the patient-specific hematological variations in general and packed volume of red blood cells (also known as the hematocrit value) in particular, here we show that the dynamics of diffusive spreading of a finite volume of human blood on a paper strip is rather universal in the healthy regime (Hematocrit ~ 30-50%) showing no dependence on the hematocrit fraction. Our results confirm the distinctive difference between the diffusive spreading of whole blood and plasma, bringing out the key influence of the cellular aggregation and consequent obstructions in the randomly distributed hierarchically structured micro-porous passages towards dictating the observed anomalous diffusion characteristics of whole blood. This aspect, in conjunction with the unique implication of a finite volume of the blood sample consistent with typical bio-analytical procedures, leads to liquid redistribution phenomenon within the porous domain, which is again influenced by the pore blockages caused by aggregated red blood cells, rendering the situation far more complex compared to Newtonian fluids. Implications of the present study may turn out to be important from several considerations, in particular, considering the fact that understanding of diffusion characteristics of blood is a mandatory prerequisite for efficient designing of paper-based bio-analytical devices. From that perspective, the present results serve as an important guideline for optimizing the dimensions of the paper strip considering the time-scales of the various stages of the analytical procedure including capillary wicking. Furthermore, these findings contribute to the fundamental understandings on spatio-temporal evolution of cellular aggregates on randomly-networked porous substrates, especially in a situation of limited supply of sample fluid. Summarily, this brings in deep science based design and analytical principles in the ambit of affordable diagnostics for public health that has by far remained to be grossly driven by operational considerations alone.

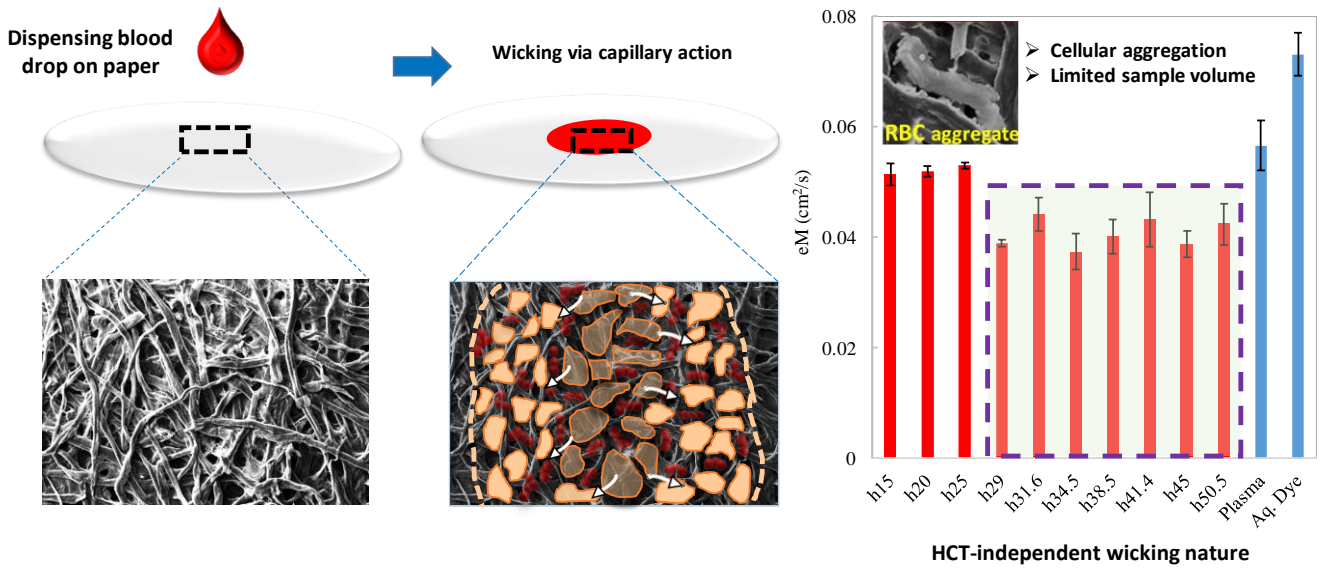


FIG. 1. Schematic representation of the experimental study showing the spreading of blood through random porous structure (Scanning electron microscopy images) of filter paper taking into account RBC aggregation and redistribution phenomenon. The effective mobility plots for different hematocrit samples are also presented showing hematocrit independent diffusive nature in the healthy hematocrit regime.

## References

- [1] Laha, Sampad, Shantimoy Kar, and Suman Chakraborty. "Cellular aggregation dictates universal spreading behaviour of a whole-blood drop on a paper strip." *Journal of Colloid and Interface Science* 640 (2023): 309-319.
- [2] Danino, Dganit, and Abraham Marmur. "Radial capillary penetration into paper: limited and unlimited liquid reservoirs." *Journal of colloid and interface science* 166.1 (1994): 245-250.
- [3] Saxton, Michael J. "Anomalous diffusion due to obstacles: a Monte Carlo study." *Biophysical journal* 66.2 (1994): 394-401.
- [4] Baskurt, Oguz K., and Herbert J. Meiselman. "Erythrocyte aggregation: basic aspects and clinical importance." *Clinical hemorheology and microcirculation* 53.1-2 (2013): 23-37.
- [5] Li, Shuaijun, Hong-hui Yu, and Jing Fan. "Modeling transport of soft particles in porous media." *Physical Review E* 104.2 (2021): 025112.

## **Sound velocity and acoustic impedance measured with picosecond laser-ultrasonics in a microfluidic channel.**

Bertrand Audoin<sup>1</sup>, François Bruno<sup>1</sup>, Jacques Leng<sup>2</sup>

<sup>1</sup>Univ. Bordeaux, CNRS, I2M, UMR 5295, F-33400 Talence, France

<sup>2</sup>CNRS, Solvay, LOF, UMR 5258, Univ. Bordeaux, F-33400 Talence, France

With an ultrafast opto-acoustic pump-probe technique we launch and record the propagation of GHz coherent acoustic phonons (CAPs) in a microfluidic channel. For this a  $X\mu\text{m}$  channel is laid on a thin metal film, serving as opto-acoustic transducer. The metal film was previously sputtered on a sapphire substrate, serving as a supporting material and as a heat sink. Femtosecond pump pulses are absorbed at the substrate-film interface along the metal skin depth. Relaxation of the over-heated electrons towards the metal lattice produces a transient stress acting as an acoustic source. After their propagation through the metal film CAPs are partly reflected at and partly transmitted through the film-microfluid interface. Firstly, we measured in time-domain the Brillouin frequency shift that results from the interaction of the probe light pulses with the transmitted acoustic wavefront propagating in the liquid medium. The velocity of CAPs with a wavelength of  $\approx 200$  nm was measured in water with various salt concentrations. Secondly, with the amplitude of the reflected CAPs we calculated the acoustic impedance of the salty solutions. By combining sound velocity and acoustic impedance we measured separately we derive both the fluid mass density and the fluid compressibility. Measurement sensitivities are discussed with numerous measurements achieved with salt concentrations ranging from 0 to 25%.

---

# Jet from a very large surface gravity wave

Ratul Dasgupta\*<sup>1</sup> and Lohit Kayal

<sup>1</sup>Indian Institute of Technology Bombay – India

## Abstract

We demonstrate that a large amplitude, modal, axisymmetric deformation in a cylindrical, radially bounded geometry can produce a sharp jet at the symmetry axis. The jet is produced purely via focussing of surface gravity waves and can be preceded by accelerations nearly three times that of gravity. A solution to the initial value problem, obtained via multiple scale analysis is found to predict the dimple which precedes the jet. In the strongly nonlinear regime, the jet evolution agrees with the theoretical model proposed by Longuet-Higgins (J. Fluid Mech. 1983)

---

\*Speaker

# A Cahn-Hilliard-Stokes model for cell aggregates dynamics

Giuseppe Sciumè<sup>1</sup>

<sup>1</sup> Institute of Mechanics and Mechanical Engineering (I2M), University of Bordeaux, 33400, Talence, France  
[giuseppe.sciume@u-bordeaux.fr](mailto:giuseppe.sciume@u-bordeaux.fr)

## I. INTRODUCTION

It is nowadays well accepted that mechanics is central to the cell functions and consequently for the behavior of multi-cellular aggregates and biological tissues. Because of the heterogeneity of cellular constituents modeling the mechanical behavior of a cell is very difficult. Very challenging is also modeling the mechanical behavior of a cell aggregate; however, in this case, if the characteristic size of the cell aggregate is larger enough with respect to the cell size, an aggregate of living cells can be modeled as a continuum. The cell aggregate continuum has a solid-like behavior at a small strain level and for relatively short characteristic times and a fluid-like behavior when submitted to sustained load and highly deformed. These solid-like and fluid-like paradigms are today quite well established and allow the scientists to classify cell types with respect to their mechanical properties which most of times are indicative of certain cell characteristics as cell-cell adhesion, cell mobility, etc. Due to this reason experiments aiming at identifying such a properties play today a pivotal role in biophysics. In this contribution a mathematical model to simulate the behavior of cell aggregates is presented and applied to model *in silico* two experiments of biophysical interest.

## 2. THE MATHEMATICAL MODEL

The cell aggregate is modeled as a mixture of two main species: the cell species,  $c$ , and the medium fluid species,  $m$ . The mixture also contains other chemical species in minor proportion, as oxygen,  $o$ , and other nutrients, which ensure the viability of the cells. If a properly representative elementary volume (REV) of mixture is defined, each point of the domain can be characterized by a certain mass fraction of cell, medium and oxygen:  $\omega_c$ ,  $\omega_m$  and  $\omega_o$  respectively.

The four governing equations of the mathematical model are:

- The mass conservation equation of the cell species;
- The mass conservation equation of oxygen;
- The mass conservation equation of the mixture;
- The momentum conservation equation of the mixture.

To close the mathematical model some constitutive relationships are also needed, namely: the stress-strain constitutive relationship; the equation for the chemical potential (which is of the Cahn-Hilliard type) and a Fick's law to model oxygen diffusion within the mixture. All these constitutive equations will be detailed in the presentation.

## 3. VISCOELASTIC RHEOLOGICAL MODEL

In the developed model the viscoelastic rheology of the cell aggregate [1] is taken into account. To this aim the definition of the stress tensor of the mixture,  $\mathbf{t}$ , includes the pressure,  $p$ , the Newtonian tensor,  $\mathbf{t}_n$ , as well as a viscoelastic tensor  $\mathbf{t}_{ve}$

$$\mathbf{t} = -p\mathbf{1} + \mathbf{t}_n + \mathbf{t}_{ve} \quad (1)$$

The Newtonian stress-stain rate relationship reads

$$\mathbf{t}_n = \mu_N \left[ \nabla \mathbf{v} + (\nabla \mathbf{v})^T \right] \quad (2)$$

where  $\mathbf{v}$  is the mixture velocity and  $\mu_N$  is the Newtonian dynamic viscosity of the mixture, which depends on the mixture composition  $\mu_N = \mu_{cN}\omega_c + (1 - \omega_c)\mu_{mN}$ .

The constitutive equation for the viscoelastic stress is of the Oldroyd-B type

$$\mathbf{t}_{ve} + \lambda_{VE} \dot{\mathbf{t}}_{ve}^{\nabla} = \mu_{VE} \nabla \mathbf{v} + \mu_{VE} (\nabla \mathbf{v})^T \quad (3)$$

where  $\lambda_{VE} = \frac{\mu_{VE}}{G_{VE}}$  ( $\mu_{VE}$  = cell viscosity and  $G_{VE}$  = cell elastic modulus) and the symbol  $\nabla$  denotes the frame invariant upper-convective derivative of a tensor field. The parameter  $\mu_{VE}$  depends on the mixture composition. In particular, it is null in the area fully consisting of medium. The relationship

$$\mu_{VE} = \mu_{cVE}\omega_c \quad (4)$$

allows to have an Oldroyd-B rheology in the cell aggregate area and to recover a Newtonian rheology in the medium areas (where  $\omega_c = 0$ ).

### 3. APPLICATION CASES

Two application cases are presented. The first application deals of tumor aggregates growing within alginate porous capsules [2], while in the second application micro-pipette aspiration of a cell aggregate is presented (see FIG. 1).

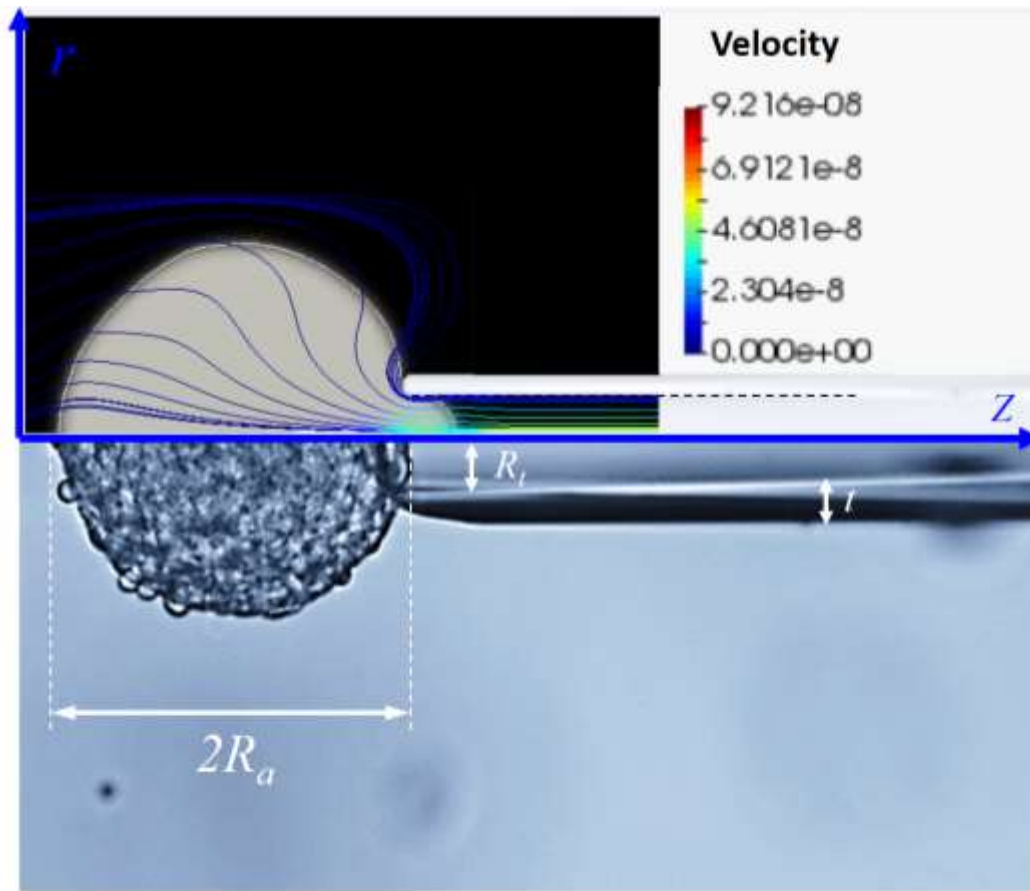


FIG. 1. Micro-pipette aspiration of a cell aggregate. Experimental image of the geometrical configuration (bottom part); numerical results after 30 minutes of aspiration (top part).

### 4. CONCLUSION

The presented results demonstrate the biophysical relevance of the proposed mathematical model and its potentialities to facilitate the interpretation of experimental results for a better understanding of mechanics of cell aggregates.

[1] Forgacs G, Foty RA, Shafrir Y, Steinberg MS. Viscoelastic properties of living embryonic tissues: a quantitative study. *Biophys J.* 1998 May;74(5):2227-34. doi: 10.1016/S0006-3495(98)77932-9. PMID: 9591650; PMCID: PMC1299566.

[2] V. Le Maout , K. Alessandri. B. Gurchenkov, H. Bertin, P. Nassoy, G. Sciumè. Role of mechanical cues and hypoxia on the growth of tumor cells in strong and weak confinement: A dual in vitro–in silico approach. *SCIENCE ADVANCES.* eaaz7130(2020).DOI:10.1126/sciadv.aaz7130

---

# The spread of a thin film and hydraulic jump formation

Roger Khayat\*<sup>1</sup>

<sup>1</sup>Department of Mechanical and Materials Engineering, Western University – Canada

## Abstract

We examine the structure of the continuous circular hydraulic jump and recirculation for a jet impinging on a disk. We use a composite mean-field thin-film approach consisting of subdividing the flow domain into three regions of increasing gravity strength: a developing boundary layer near impact, an intermediate supercritical viscous layer, and a region comprising the jump and subcritical flow. Unlike existing models, the approach does not require any empirically or numerically adjusted boundary conditions. We demonstrate that the stress or corner singularity for a film draining at the edge is equivalent to an infinite slope of the film surface, which we impose as the downstream boundary condition. The model is validated against existing experiment and numerical simulation of the boundary-layer and Navier-Stokes equations. We find the flow in the supercritical region remains insensitive to the change in gravity level but is greatly affected by viscosity. The existence of the jump is not necessarily commensurate with the presence of recirculation, which is strongly dependent on the upstream curvature and steepness of the jump.

---

\*Speaker

# Grid dependent collapse in Volume of Fluid simulations of atomisation of a dense pulsating jet: A solution with the Manifold Death method

Y. Kulkarni<sup>1</sup>, R. Villiers<sup>1</sup>, C. Pairetti<sup>1</sup>, M. Crialesi-Esposito<sup>2</sup>, S. Popinet<sup>1</sup> and S. Zaleski<sup>1,3</sup>

<sup>1</sup> Institut Jean le Rond d'Alembert, Sorbonne Université and CNRS, 75005 Paris, France.

<sup>2</sup> KTH Royal Institute of Technology, 11428 Stockholm, Sweden.

<sup>3</sup> Institut Universitaire de France, Institut Jean le Rond d'Alembert, F75005 Paris, France.

Jet atomisation is a multi-scale phenomenon and hence a challenging problem for numerical simulations, even in isothermal and incompressible flow ([1], [2]). Despite being computationally challenging, to capture the physics of such a multi-scale problem, we perform the direct numerical simulations (DNS) using the Volume of Fluid (VoF) method. We simulate a dense pulsating cylindrical liquid oil jet injected into a stagnant air phase with Reynolds number  $Re = 5800$ , Weber number  $We = 5555$  and density ratio  $r = 28$  using the VoF method and octree adaptive mesh refinement with the Basilisk code. We achieve a grid refinement higher than 900 cells per initial jet diameter. This is, to our knowledge, the most detailed simulation, including this type of flow. Through our detailed simulations, we observe many underlying mechanisms, including the effect of pulsation, characteristic sheet perforation due to droplet impact, and sheet rupture due to stretching and thinning. As shown in figure 1, we obtain a bimodal distribution for the probability density function, with two peaks in droplet sizes. Surprisingly, the position of the peak corresponding to the smaller droplets shift uniformly towards smaller scales as the grid size  $\Delta$  is decreased, indicating the grid dependency of the mechanisms involved and hence, absence of statistical convergence. There is, however, still a convergence seen in the tail region of the histogram of droplet sizes which shows that the largest of the droplets have converged. Thanks to the post-processing capabilities of our Basilisk code, in figure 2 the interface coloured by the numerical curvature revealed that the sheet perforation was the likely culprit for the grid-dependent peak corresponding to the small droplets. We then use the Manifold Death method [3], which allows us to control the topological changes of thin structures in the flow. We first detect the weak spots and thin ligaments using the signature cubes and then punch a hole artificially. We specify the critical size (must be greater than the grid size) of the signature cube independently from the grid size. With the improved VoF with Manifold death, we decrease the grid dependency and obtain a better statistical convergence for the droplet size distribution. Our results thus suggest that the traditional VoF method, even with infinite computational power, will not provide a statistical convergence. However, the use of the Manifold Death method can help decrease the grid dependency and improve statistical convergence. These findings have important implications for the study of jet atomisation and can pave the way for more accurate simulations in the future. This is to best of our knowledge the first ever statistical convergence obtained in resolved VoF simulations for this type of atomisation flow.

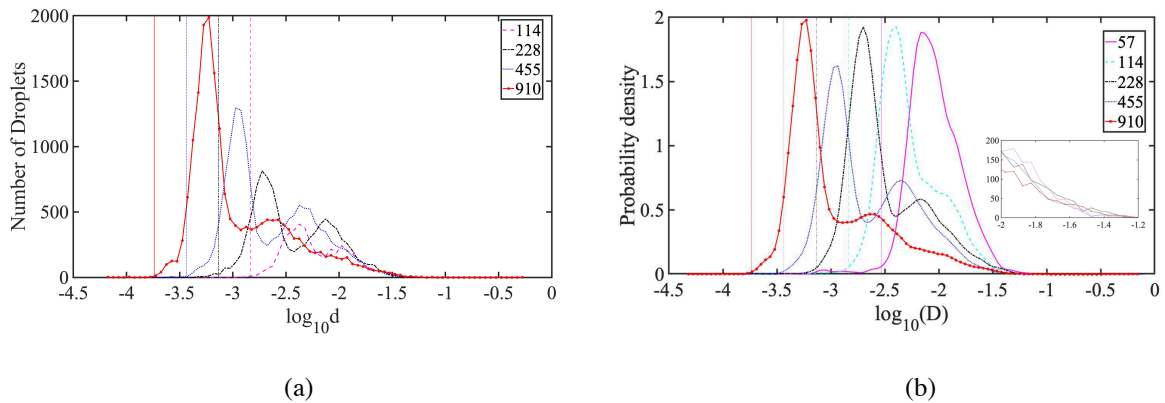


FIG. 1. The grid dependent statistics for the VoF only simulations. (a) The histogram showing the droplet size distribution. (b) The probability density function for the droplet sizes for the same histogram. Legend indicates the number of grid points per initial diameter for both the plots.

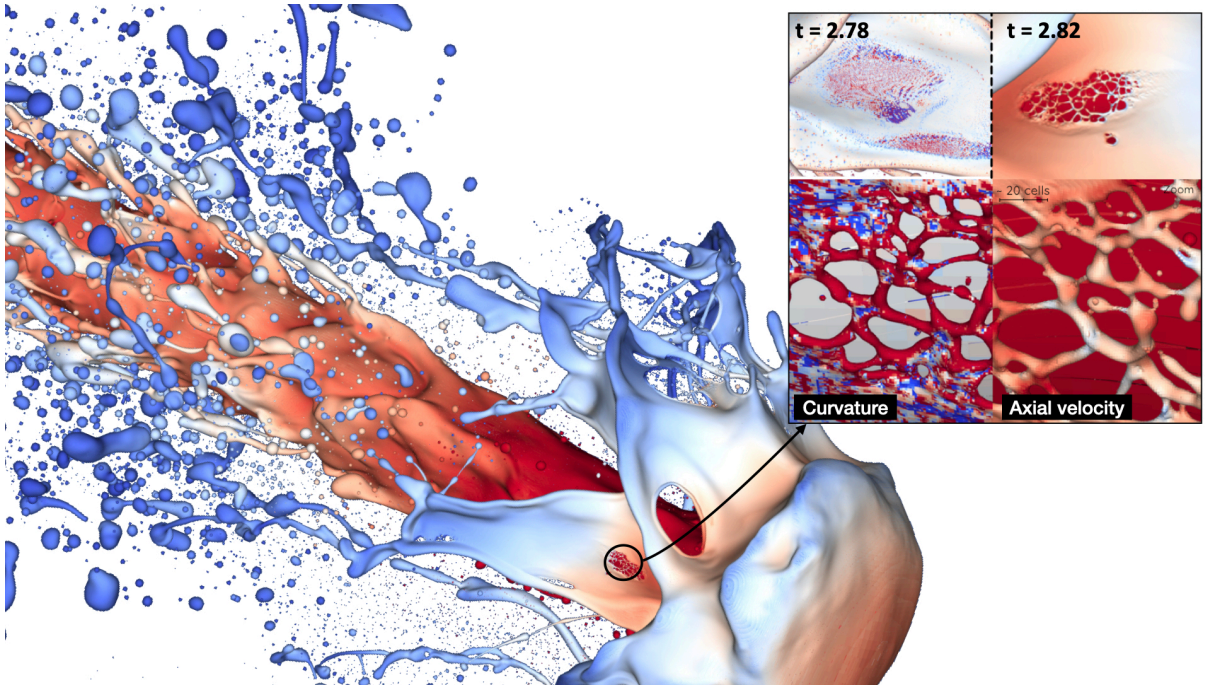


FIG. 2. Numerical sheet rupture for the VoF only simulations. In the inset, the background coloured by the curvature shows oscillations in the numerical curvature giving rise to ligament network that scale with the grid size. These then result in the grid dependent droplets.

### References:

- [1] R. D. Reitz, F. V. Bracco, Mechanism of atomization of a liquid jet, *Physics of Fluids*, 1982.
- [2] M. Gorokhovski, M. Herrmann, Modeling Primary Atomization, *Annual Review of Fluid Mechanics*, 2008.
- [3] Leonardo Chirco, Jacob Maarek, Stéphane Popinet, and Stéphane Zaleski. Manifold death : A volume of fluid implementation of controlled topological changes in thin sheets by the signature method. *Journal of Computational Physics*, 2022.

# Ultrasound resonance in a coflow exposed to bulk acoustic waves

Ashis Kumar Sen<sup>1</sup> and Sazid Zamal Hoque<sup>2</sup>

<sup>1</sup>Department of Mechanical Engineering, MNBU, IITM, 600036, Chennai, India, ashis@iitm.ac.in

<sup>2</sup>Department of Mechanical Engineering, MNBU, IITM, 600036, Chennai, India, saqidzama@gmail.com

The physics of manipulation of micro-objects suspended in a liquid exposed to bulk acoustic waves (BAW) is well suited for microfluidics applications [1]. Typically, the microchannel width is kept equal to the half-wavelength of the sound wave in a liquid so that the pressure nodal plane (NP) is formed at the center, and the condition is known as the ultrasonic resonance mode. The particle experiences maximum acoustic radiation force at the resonance mode and thereby moves toward the NP. Such resonance mode can also be established in a two liquids coflow domain for manipulation of droplets and particles [2]. However, there is a discontinuity in the density and speed of sound across the immiscible liquid interface, which can significantly alter the acoustic field, hence the resonance condition of the two liquids system. Here, a systematic study regarding the ultrasonic resonance of two liquid systems exposed to BAW is presented via numerical simulations and experiments.

A three-dimensional numerical model is developed to predict the acoustic pressure eigenmodes of a two liquids domain for a better understanding of the acoustic resonance mode of the system. The Helmholtz equation is given by  $\nabla^2 p_1 = -k_0^2 p_1$  is solved to determine the acoustic eigenmodes,  $p_1 = \tilde{p}_1(r)e^{-i\omega t}$  by considering appropriate boundary conditions. The first-order velocity fields and normal stresses are continuous at the fluid-fluid interface and are implemented to obtain the background one-dimensional pressure field as [3],

$$p^b = p_{in}[R\cos(ky + \omega t) + \cos(\omega t - ky)] \quad (1)$$

where  $R$  is the reflection co-efficient defined as  $R = (Z_1 - Z_2)/(Z_1 + Z_2)$ ,  $Z_1$  and  $Z_2$  are respectively the characteristic acoustic impedance in liquid 1 and liquid 2. Here,  $p_{in}$  is the amplitude of the incoming pressure wave, which is of the order  $\sim 1$  MPa, corresponding to the resonating frequency of 1-2 MHz range. The microchannel wall boundary conditions have a significant effect on the resonance modes. Depending on the substrates used in the device (silicon and borosilicate glass), the hard wall boundary is considered as  $\mathbf{n} \cdot \nabla p_1 = 0$  where  $\mathbf{n}$  is the unit normal vector at the interface. Further, experiments are performed to see the migration of particles to the center of the microchannel via a frequency sweep.

Numerical simulations are performed to obtain the acoustic eigenmodes of a coflow domain of width,  $w = 375 \mu m$ , height,  $h = 200 \mu m$ , and length  $l = 2$  mm. The amplitude of the background pressure field given by eqn. (1) is taken as,  $p_{in} = 5.965$  MPa, and the Helmholtz equation is solved in the frequency domain. The variation of maximum pressure amplitude ( $P_{max}$ ) as a function of actuation frequency for different stream width ratios is presented in FIG. 1. It is found that when the speeds of sound and densities of the liquids are comparable, the resonating frequencies at which the maximum pressure amplitude (i.e., half wave resonance) is obtained converge to a single value and are independent of the stream width ratios. The resonating frequency for mineral oil – olive oil case is 1.90 MHz. When the speeds of sound or densities differ significantly, i.e., olive oil – silicone oil combination, the resonance frequency shifts in a range depending on the stream width ratio. The resonating frequency for the silicone oil–olive oil combination lies in the range of  $f_{si} = 1.375$  MHz and  $f_{ol} = 1.970$  MHz.

Further, transient simulations are performed to show the particle focusing toward the nodal plane by coupling the acoustic pressure field from the steady state simulations (neglecting the fluid's velocity) with the Particle Tracing Module in COMSOL. The model for the particle dynamics considers primary acoustic radiation force due to the acoustic pressure and velocity fields at half-wave resonance and the drag force acting on the particles. The drag force acting on the particles is modeled using the linear Stokes drag formula. The primary acoustic radiation force acting on the particles due to scattering of the acoustic wave from the particle surface is defined as,  $\mathbf{F}_p = -2\pi R^3 \nabla \left[ f_1 \frac{1}{3\rho_f c_f^2} \langle p_{in}^2 \rangle - \frac{1}{2} f_2 \rho_f \langle v_{in}^2 \rangle \right]$ , where  $f_1$  and  $f_2$  are the monopole and dipole coefficients defined as,  $f_1 = 1 - ((\rho_f c_f^2)/(\rho_p c_p^2))$  and  $f_2 = 2(\rho_p - \rho_f)/(2\rho_p + \rho_f)$  [4]. The particles are initially randomly positioned in the liquid

containing the pressure NP and get focused at the pressure NP when the system is exposed to BAW, as shown in FIG. 1(a)ii and FIG. 1(b)ii. Next, we experimentally verify ultrasonic resonance conditions in the different coflow systems by observing the particle migration towards the pressure NP.

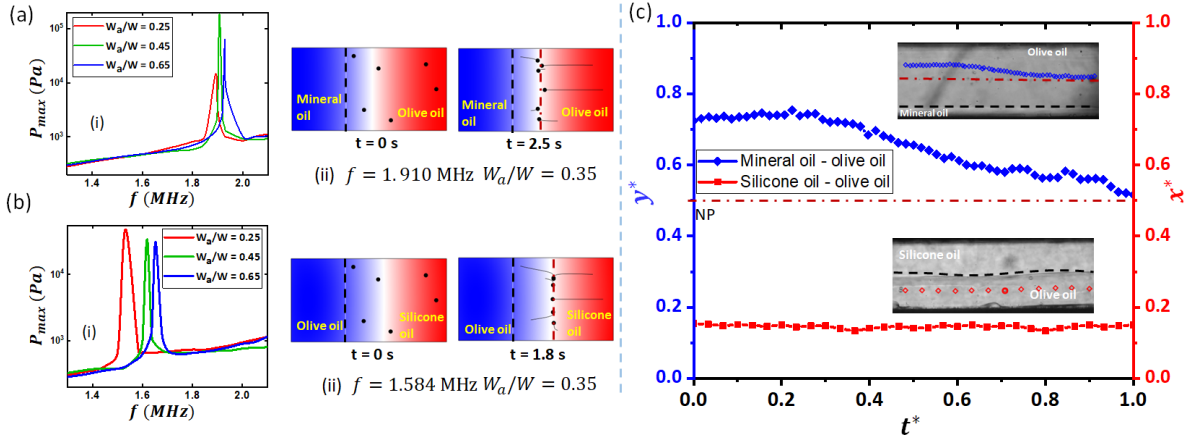


FIG. 1. Numerical simulation results showing (i) the variation of maximum acoustic pressure field amplitude with actuation frequency for different width ratio of the streams and (ii) particle focusing at the nodal plane due to acoustic waves for  $(W_a/W) = 0.35$  (a) Mineral oil – olive oil, (b) Olive oil- silicone oil, and (c) Focusing/non-focusing of the microbeads towards the center with time in different coflow systems, insets in (c) show the experimental images of the particle motion.

Experiments are performed with different coflow systems by suspending the polystyrene particle in the liquid having a higher stream width covering the center of the channel. The system is then exposed to BAW, and the actuating frequency is varied to achieve a half-wave resonance mode where the particles migrate toward the NP. The experimental images of particles focusing in the different immiscible coflow systems after applying BAW with a power of 5.49 W and the particle trajectories with time are presented in FIG. 1(c). The interface deformation and acoustic relocation are suppressed by satisfying the low acoustocapillary number condition,  $Ca_{ac} < 1$  [5]. In each coflow system, the actuation frequency is varied from 1.300 to 2.900 MHz to determine the resonating frequency at which the particle focusing at the pressure NP is achieved. In the mineral oil–olive oil case, having a comparable speed of sound value, the particles are focused at the microchannel center showing the formation of an NP at a resonating frequency of 1.905 MHz. In the case of the olive oil-silicone oil system, owing to a marked difference in the speeds of sound in the liquids, the resonating frequency is sensitive to the variation of stream width ratio (see FIG. 1(b)i). In such cases, particle focusing is not observed owing to the variation of the resonating frequency to stream width ratio, and it is also sensitive to kHz range variation. However, the resonance modes of any two fluids domain can be easily predicted using the 3D numerical model.

In summary, ultrasonic resonance in coflow systems with a pair of immiscible liquids in a microchannel exposed to BAW is studied. We discovered that resonance could be achieved in the such system by actuating at a single resonating frequency whose value is governed by the ratio of sound speeds, densities, and the widths of the liquids. The resonating frequency of a system with liquids of equal speeds of sound and densities is independent of the width ratio. Further, the resonating frequency of a coflow system with unequal speeds of sound and densities is proportional to the stream width ratio.

- [1] J. Friend and L. Y. Yeo, *Microscale Acoustofluidics: Microfluidics Driven via Acoustics and Ultrasonics*, Rev. Mod. Phys. **83**, 647 (2011).
- [2] E. Hemachandran, T. Laurell, and A. K. Sen, *Continuous Droplet Coalescence in a Microchannel Coflow Using Bulk Acoustic Waves*, Phys. Rev. Appl. **12**, 1 (2019).
- [3] T. Baasch and J. Dual, *Acoustic Radiation Force on a Spherical Fluid or Solid Elastic Particle Placed Close to a Fluid or Solid Elastic Half-Space*, Phys. Rev. Appl. **14**, 1 (2020).
- [4] H. Bruus, *Acoustofluidics 7: The Acoustic Radiation Force on Small Particles*, Lab. Chip. **12**, 1014-1021 (2012).
- [5] E. Hemachandran, S. Z. Hoque, T. Laurell, and A. K. Sen, *Reversible Stream Drop Transition in a Microfluidic Coflow System via On Demand Exposure to Acoustic Standing Waves*, Phys. Rev. Lett. **127**, 134501 (2021).

---

# The nature of branching in electrohydrodynamic instability and its comparison with Rayleigh Taylor instability of a viscoelastic fluid

B. Dinesh\*<sup>1</sup> and R. Narayanan<sup>2</sup>

<sup>1</sup>Indian Institute of Technology [BHU Varanasi] – India

<sup>2</sup>University of Florida [Gainesville] – United States

## Abstract

An electric field imposed on a bilayer of fluids that are stable and stratified in the presence of gravity leads to an instability manifested by interfacial deflections. For the case of a perfect conductor underlying a perfect dielectric, an analytical expression obtained from weak nonlinear analysis shows that sinusoidal deflections can only lead to subcritical breakup. While this expression indicates that there is a transition wave number below which supercritical saturation ought to occur, it can be shown that such wave numbers cannot be geometrically accessed, thus precluding any supercritical saturation to steady waves. In contrast to electrohydrodynamic instability, the Rayleigh–Taylor instability of a laterally unbounded linear viscoelastic fluid must always result in saturated steady waves. The branching behavior upon instability to sinusoidal disturbances is determined by weak nonlinear analysis. This analysis leads to the counterintuitive observation that a laterally unbounded layer must always result in saturated steady waves. However, the analysis also shows that the subcritical breakup in a viscoelastic fluid can only occur if the layer is laterally bounded below a critical horizontal width.

---

\*Speaker

---

# Direct Numerical Simulation of Cavitation Inside Blood Vessels

Ahmed Basil Kottilingal\*<sup>1</sup> and Stéphane Zaleski\*

<sup>1</sup>Sorbonne université - Faculté des Sciences et Ingénierie – Sorbonne Université – France

## Abstract

Ultrasound can be used to create controlled oscillations of microbubbles within blood vessels, modifying the vessel wall permeability in a process called sonoporation. This technique has potential applications in gene therapy and targeted drug delivery for cancer treatment. In this study, our focus is on the response of coated bubbles to high frequency ultrasound waves, using an all-mach formulation to simulate a compressible multiphase flow of bubble and liquid. Our multiphase flow solver, based on front tracking method, incorporates surface tension and viscous forces in the formulation. The interaction between a cavitating bubble and a blood vessel is captured using Immersed Boundary Method (IBM) models. The fluid properties, undeformed vessel radius, and vessel compliance parameters are matched with the real case scenario of a blood capillary. The study focuses on a parametric study of the initial bubble diameter and ultrasound characteristics in determining the optimal choice for targeted drug delivery.

---

\*Speaker

---

# A second-order coupling of Carman-Koseny expression with Navier-Stokes equations for modelling fluid-structure interactions

S Venkatesan Diwakar\*<sup>1</sup>

<sup>1</sup>Jawaharlal Nehru Centre for Advanced Scientific Research – India

## Abstract

The process of fluid-structure interaction is an inevitable part of many natural and industrial processes. In many cases, this interaction could be the sole cause of fluid flow and the associated manifestations. The interactions between the solid and fluid could range from one-way forcing to two-way coupling, and understanding their influence is essential in applications like moving automobiles, naval structures, combustion chambers etc. In this regard, various numerical procedures have been employed, and the complexity of such calculations increases when the solid body has its own dynamics. One of the conventional ways often utilized for this purpose is the arbitrary Eulerian-Lagrangian method which involves body-conforming grids. However, this method is computationally expensive and in cases of significant solid displacement, re-meshing becomes essential. One can resort to Eulerian-Eulerian approaches such as the "immersed boundary method" to overcome such issues. The method uses a non-conformal Cartesian grid that spans over the whole computational domain, and the solid structure is represented by Lagrangian marker points. The effect of the singular force acting on the markers is spread to the surrounding grid points using discrete Dirac delta functions. This method was originally developed for handling flows with immersed elastic boundaries, but subsequent modifications have made it capable of handling flows with rigid boundaries. The major issue here is the generation of unphysical spurious pressure field oscillations for moving or oscillating bodies mainly due to the imposition of the forcing term on discrete points. Alternatively, one can employ the fictitious-domain method, where the presence of the solid body is characterized by a volumetric source term added to the governing momentum equation. The solid body is considered as an immersed volume in the fluid, and a volumetric resistance term emulates it in such a way that the permeability approaches infinity for the fluid phase and is zero for the fully solid region. In this method, the smooth transition from the fluid medium to the solid depends upon the manner of approximating the volumetric forcing term. One way of approximation is through the Carman-Koseny expression. The present work uses this approach in conjunction with a cut-cell-type interpolation to arrive at a second-order accurate solution procedure. In the current talk, the detailed steps involved in the approach are systematically presented, and the efficacy of the approach is exemplified using various benchmark problems. The method opts for a volumetric forcing implementation that eliminates spurious oscillations. Also, the numerical implementation of this methodology is comparatively easier than other conventional methods like the immersed boundary.

---

\*Speaker

# Rheology of soft attractive microcapsules

Hugues Bodiguel<sup>1</sup>, Mehdi Maleki<sup>1</sup>, Clément de Loubens<sup>1</sup>

<sup>1</sup>Univ. Grenoble Alpes, CNRS, Grenoble-INP, LRP UMR 5520, Grenoble, France

**Topic(s):** Low Reynolds suspensions: from single particle to collective behavior

**Key words:** Micro-capsule, suspension, gel

## Abstract:

We are interested in the rheological properties of dense suspensions of deformable particles because of their biological (e.g. blood) and industrial (e.g. microcapsules) interest. We study as a system microcapsules of about 100 micrometers composed of a membrane obtained by complexation of polyelectrolytes at the water-oil interface (Xie et al., *Soft Matter*, 2017). Homogeneous suspensions in size and mechanical properties are generated through a membrane emulsification process. In addition, the elastic properties of the particles are characterized through automated measurement of their deformation in a microfluidic elongational flow chamber (Maleki et al. *Chem. Eng. Sci.*, 2021). The rheological properties of the suspensions are characterized in oscillatory rotational rheometry, steady-state rheometry, and shear reversal experiments for volume fractions ranging from 20 to 55%.

Surprisingly, the suspensions obtained show a Bingham-like behavior with a flow threshold for volume fractions of 25%. The threshold increases with the volume fraction. Oscillation measurements show that the elastic modulus of the suspension increases with time, signature of aggregations in the system over time, cf figure showing clusters of microcapsules. The elastic properties of the microcapsules have little influence on the results. The viscoelastic behavior of the suspension after a pre-shearing, in order to break the clusters of capsules, is characteristic of a behavior of attractive colloidal suspensions (Trappe and Weitz, *PRL*, 2000). We perform various shear reversal experiments. These experiments highlight that the flow threshold is associated with the formation of a microstructure under flow. Above the threshold, the behavior of the microcapsule suspension is very similar to that of rigid sphere suspensions with lubricated contacts.

In conclusion, the microcapsule system formed by polyelectrolyte complexation has attractive colloidal particle behavior for particle sizes of several hundred micrometers. The flow threshold is related to underflow structuring, while above this threshold the suspension behaves as a suspension of non-crushing spheres.

Perspectives of this work deal with direct measurement of the attractive force between micro-capsule, and is currently being performed using a dedicated micropipette suction sensor. Preliminary results confirm the order of magnitude and the range of the attractive interactions, but also evidence more complex phenomena such as a strong repulsion when the particles enter into contacts.

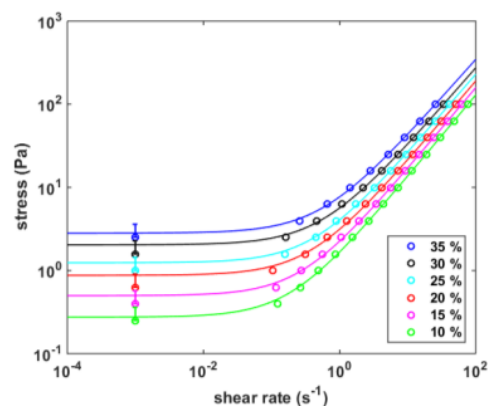
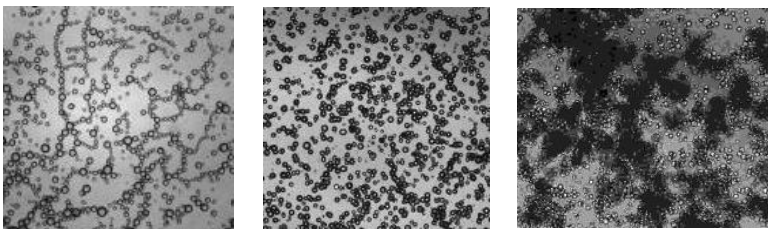


**Figure 1:** From left to right: image of the suspension of microcapsules under an electric field; in a high permittivity silicone oil (AK1000); in a low permittivity silicone oil (AP1000); flow curve of suspensions of microcapsules in AK1000 at various volume fraction. The suspensions exhibit a yield stress at low shear rates, even at very low volume fraction.

# Activity induced rigidity of liquid droplets.

Hamid KELLAY

*Laboratoire Ondes et Matière d'Aquitaine (LOMA)*

[hamid.kellay@u-bordeaux.fr](mailto:hamid.kellay@u-bordeaux.fr)

## **Abstract**

Encapsulating active Janus particles within a drop renders it more resistant to deformation. This drop is deformed under the action of an extensional flow. Such deformation is primarily resisted by the drop interfacial tension. When the particles are active under the action of laser illumination, the deformation decreases signaling an increase in effective tension or Laplace pressure. This increase is attributed to the activity of the particles. Our results using numerous drop sizes, particle number densities, and active velocities show that the obtained increase agrees surprisingly well, over an extended range, with a standard expression for the pressure engendered by an ensemble of active particles, proposed years ago but not tested yet in three dimensions.

# **Three Phase Systems under Electric Field: From 'Kissing' Droplets to Threading Glass beads**

Dipankar Bandyopadhyay

Professor, Department of Chemical Engineering & Centre for Nanotechnology,  
Indian Institute of Technology Guwahati

## **Abstract**

Droplets or particles while floating or impacting inside/on a fluid or gaseous medium manifest interesting flow morphologies that has connection to various self-organizing natural processes. For example, a collection of glass microbeads suspended inside a liquid may join as a thread under the influence of an external field and change the local rheology of a fluid while a pair of immiscible droplets may indulge in symmetric to asymmetric 'kissing' phenomena under similar circumstances. Exploration of the fundamentals of such systems are significantly relevant from the translational point of view because they can be utilized to tune the rheology of a microfluidic flow non-invasively or a controlled bridging and breaking of a pair of droplets can facilitate a non-invasive protocol for delivery/exchange of materials. This talk will cover a collage of such systems which will also divulge the recipes to develop some metastable flow structures such a toroids and double toroids among others.

# On-demand collective and cooperative dynamics of dense active systems

L. Alvarez, E. Sesé, D. Levis, Pagonabarraga, L. Isa.

The emerging collective behaviour characteristic of biological systems relies on the ability of their single units to effectively interact and exchange information. Active colloids present a versatile model system to understand the underlying physics of this phenomenon. However, current experimental systems are limited to the accessible emerging collective phases due to design constraints.

Here, we explore the collective and cooperative dynamics of two populations of Janus particles with different mobility under actuating AC electric fields [2]. We first explore the behaviour of each population in the dilute and dense regimes. We find a transition from a disordered phase to polar cluster mediated by the field frequency and independent of the particle's mobility. We justify this effect by the electrohydrodynamic and dipole interactions that mediate the particle potentials and the alignment events. We then study the behaviour of mixtures with the two populations, where we find effective mobility enhancement of the slow species due to the interaction with the fast particle's polar clusters. We find good agreement using a Vicsek-like model [3] accounting for an effective alignment force related to the frequency of the applied electric field. The experimental design allows for fine-parameter control, with the potential for future study of a broader range of group dynamics.

[1] L. Alvarez, E. Sesé, D. Levis, Pagonabarraga, L. Isa. (in preparation)

[2] A. Martín-Gómez, D. Levis, A. Díaz-Guilera, I. Pagonabarraga, *Soft Matter*, **14**, 2610-2618 (2018)

# Author Index

- Alvarez Laura, 49  
Amarouchene Yacine, 27  
Arrigoni Michel, 8  
Audoin Bertrand, 34
- Bandyopadhyay Dipankar, 48  
Baresch Diego, 14  
Baret Jean-Christophe, 24  
Beneyton Thomas, 24  
Biswas Gautam, 2, 3  
Bodiguel Hugues, 46  
Brunet Philippe, 18, 19
- Chakraborty Suman, 25, 32, 33  
Chen Xiangbin, 15, 16  
Chraïbi Hamza, 17  
Crialessi-Esposito Marco, 39, 40
- Das Sovan Lal, 20  
Dasgupta Ratul, 35  
Dash Susmita, 7  
De Loubens Clement, 46  
Delabre Ulysse, 17  
Delville Jean-Pierre, 17  
Dietze Georg, 23  
Dinesh B., 43  
Diwakar S Venkatesan, 45
- Farutin Alexander, 21, 22  
Fuster Daniel, 8, 15, 16
- Ghosh Uddipta, 4, 5, 28, 29  
Ghulam Rabbani, 26  
Giot Antoine, 17  
Guerin Thomas, 17
- Hoque Sazid Zamal, 41, 42
- Jha Aditya, 27
- Kar Shantimoy, 32, 33  
Karan Pratyaksh, 28, 29  
Kayal Lohit, 35  
Kellay Hamid, 47  
Khayat Roger, 38  
Kottilingal Ahmed Basil, 44
- Kulkarni Yash, 39, 40  
Kumar Srijan, 7
- Laha Sampad, 25, 32, 33  
Le Borgne Tanguy, 28, 29  
Lin Zi, 24
- Maleki Mehdi, 46  
Martin Nicolas, 24  
Meheust Yves, 28, 29  
Michelin Sebastien, 9, 10  
Misbah Chaouqi, 20–22  
Mohan Ananthan, 11–13  
Mu Lizhong, 23
- Naidu Deekshith, 7  
Narayanan R., 43  
Nayak Ananta Kumar, 20
- Pairetti Cesar, 39, 40  
Pal Ashwani, 2, 3  
Panigrahi Pradipta, 31  
Petit Julien, 17  
Popinet Stéphane, 39, 40
- Ray Bahni, 26  
Roy Anubhab, 30
- Sahu Kirti, 6  
Saini Mandeep, 8, 15, 16  
Saiseau Raphael, 17  
Salez Thomas, 1, 27  
Santra Somnath, 21, 22  
Sciumè Giuseppe, 36, 37  
Sen Ashis, 41, 42
- Tanné Erwan, 8  
Tomar Gaurav, 11–13
- Ueno Ichiro, 23
- Viliers Raphael, 39, 40  
Vinze Prathmesh, 9, 10
- Yoshikawa Harunori, 23
- Zaleski Stéphane, 8, 15, 16, 39, 40, 44  
Zoueshtiagh Farzam, 23